International Journal of Disaster Risk Reduction 77 (2022) 103078

Contents lists available at ScienceDirect

International Journal of Disaster Risk Reduction

journal homepage: www.elsevier.com/locate/ijdrr

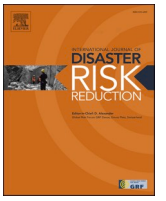

# Spatiotemporal disparities in regional public risk perception of COVID-19 using Bayesian Spatiotemporally Varying Coefficients (STVC) series models across Chinese cities

Chao Song [a,b,c], Hao Yin [d,e,**], Xun Shi [b], Mingyu Xie [c], Shujuan Yang [a], Junmin Zhou [a], Xiuli Wang [a,c], Zhangying Tang [f], Yili Yang [c], Jay Pan [a,c,*]

[a] HEOA Group, West China School of Public Health and West China Fourth Hospital, Sichuan University, Chengdu, Sichuan, 610044, China
[b] Department of Geography, Dartmouth College, Hanover, NH, 03755, USA
[c] Institute for Healthy Cities and West China Research Centre for Rural Health Development, Sichuan University, Chengdu, Sichuan, 610041, China
[d] Department of Economics, University of Southern California, CA, 90089, USA
[e] School of Population and Public Health, University of British Columbia, BC, V6T 1Z3, Canada
[f] State Key Laboratory of Oil and Gas Reservoir Geology and Exploitation, School of Geoscience and Technology, Southwest Petroleum University, Chengdu, Sichuan, 610500, China

ARTICLE INFO

*Keywords:*
Regional public risk perception
Multi-level spatiotemporal heterogeneity
Spatiotemporal non-stationary regression
STVC
Internet search engine
COVID-19

ABSTRACT

Regional public attention has been critical during the COVID-19 pandemic, impacting the effectiveness of sub-national non-pharmaceutical interventions. While studies have focused on public attention at the national level, sub-national public attention has not been well investigated. Understanding sub-national public attention can aid local governments in designing regional scientific guidelines, especially in large countries with substantial spatiotemporal disparities in the spread of infections. Here, we evaluated the online public attention to the COVID-19 pandemic using internet search data and developed a regional public risk perception index (PRPI) that depicts heterogeneous associations between local pandemic risk and public attention across 366 Chinese cities. We used the Bayesian Spatiotemporally Varying Coefficients (STVC) model, a full-map local regression for estimating spatiotemporal heterogeneous relationships of variables, and improved it to the Bayesian Spatiotemporally Interacting Varying Coefficients (STIVC) model to incorporate space–time interaction non-stationarity at spatial or temporal stratified scales. COVID-19 daily cases (median contribution 82.6%) was the most critical factor affecting public attention, followed by urban socioeconomic conditions (16.7%) and daily population mobility (0.7%). After adjusting national and provincial impacts, city-level influence factors accounted for 89.4% and 58.6% in spatiotemporal variations of public attention. Spatiotemporal disparities were substantial among cities and provinces, suggesting that observing national-level public dynamics alone was insufficient. Multi-period PRPI maps revealed clusters and outlier cities with potential public panic and low health literacy. Bayesian STVC series models are systematically proposed and provide a multi-level spatiotemporal heterogeneous analytical framework for understanding collective human responses to major public health emergencies and disasters.

* Corresponding author. HEOA Group, West China School of Public Health and West China Fourth Hospital, Sichuan University, Chengdu, Sichuan, 610044, China.
** Corresponding author. Department of Economics, University of Southern California, CA, 90089, USA.
*E-mail addresses:* chaosong@scu.edu.cn (C. Song), yinhao@usc.edu (H. Yin), panjie.jay@scu.edu.cn (J. Pan).

https://doi.org/10.1016/j.ijdrr.2022.103078
Received 24 February 2022; Received in revised form 24 May 2022; Accepted 24 May 2022
Available online 29 May 2022

## 1. Introduction

In the face of major public health emergencies and social disasters, public attention and public risk perception can affect human behavior choices, which is, therefore, essential for crisis management [1,2]. The ongoing COVID-19 (Corona Virus Disease 2019) pandemic has caused millions of deaths and inflicted profound consequences on social and economic development worldwide [3,4]. Due to the growing variants of SARS-CoV-2, the unequal vaccine distribution worldwide, as well as the adjustment of prevention and mitigation strategies, non-pharmaceutical interventions (NPIs), including personal protective equipment and social distancing strategies, can be relied on as effective manners to control the spread of COVID-19 worldwide [5,6]. The adoption of NPIs has remained a priority for many countries when a fast-spread variant of COVID-19 emerges, even for those with a high level of vaccination [7,8]. As the effectiveness of NPIs depends on population-level spontaneity, cooperation, and fast acquisition of updated information, it is critical to determine how people respond to the information on the pandemic as well as intervention policies worldwide [9,10], both in developed countries and developing countries [11,12].

The collective human attention to COVID-19 can impact the effectiveness of regional NPIs in terms of the timing and implementation of prevention measures to further influence the actual progress of the pandemic [9,10]. The Internet has played a pivotal role during this unprecedented pandemic and serves as the predominant source for the general public to acquire news and other health- and disease-related information [13–16]. With the explosion of modern internet information, human attention to crucial information is of critical importance [17]. Internet search engine products, such as Google Trends and Baidu Index, have been widely used as indicators to illustrate the collective public attention to COVID-19 [18–20]. In China, infoveillance studies based on the Baidu Index identified two critical periods for early-stage disease control when national public attention was low [9,21]. In the United States, infoveillance studies using Google Trends showed that the initial public attention to COVID-19 at the national level was limited, short-lived, and even decreased during the critical period when increasingly strong control strategies were put in place [13,22]. Using Google Trends, similar findings reflective of relatively low-level public attention were also reported globally in both early infected developed and developing countries [9,10,12]. However, most COVID-19 infodemiology studies using internet search engine data are currently conducted at the national level [9,10,13,21,22].

There is an urgent need to conduct sub-national level evaluations on the collective human attention for better informed local interventions. Spatial heterogeneity can lead to substantial local variations in COVID-19 timing and severity [23,24]. Research suggests that a region-by-region social distancing measure played an essential role in mitigating the COVID-19 pandemic [25,26]. A one-size-fits-all strategy for COVID-19 based on such national-level findings could be socially and economically unfeasible [27,28], underlining the need to consider spatial heterogeneity (disparities) across different levels of administrative divisions [25,29]. Going beyond the concept of spatial heterogeneity, an increased number of studies have emphasized the necessity of an integrated perspective of utilizing spatiotemporal heterogeneity to facilitate differential control of COVID-19 [30,31], especially in large countries in terms of both the landscape and population sizes, such as the US [32,33] and China [34]. Existing spatiotemporal studies on COVID-19 lack the insights provided by analyses of fine-scale data of regional public attention, defined as the collective human attention at the geospatial level.

More importantly, the level of regional public attention itself might not always reflect the level of regional public risk perception due to the neglect of actual local pandemic risk across different locations [35,36]. For example, low attention areas with high risks of COVID-19 may indicate a relatively lower risk perception to COVID-19, while high attention areas with low risks could reveal an excessive risk perception, which can cause potential public panic and thereafter trigger substantial economic loss and social unrest [37,38]. Identifying the regions with unmatched public attention and local risk provides information on the priorities of pandemic interventions within a country or a large study area. Therefore, beyond regional public attention, it is of great concern to investigate variations in regional public risk perception across space and over time. However, no available studies have identified the various levels of both regional public attention and regional public risk perception of COVID-19 while taking into account the spatiotemporal heterogeneity.

Unlike traditional indicators of public risk perception based on the population survey [2,35,38], the regional public risk perception can be characterized by estimating the spatially heterogeneous associations between regional public attention and the severity of the local pandemic. Numerous studies using different online platforms have shown the significant association between online public attention and COVID-19 reported cases across various countries around the globe [9,12] as well as within specific countries such as the US [22] and China [39,40]. It is noteworthy that socioeconomic conditions could also affect the regional public attention arising from internet search engines, since the dissimilarities in economic conditions would lead to disparities in the amount of people searching the Internet [41]. Amidst densely populated and economically developed areas, people paid more attention to the dynamics of infections through the Internet [42]. Research also showed that socioeconomic factors were associated with online searches (Google Trends) about health and epidemics [43,44]. Additionally, restrictions on population mobility may lead to increased attention to the Internet [45,46]. For instance, during the very beginning of the outbreak in China, the movement of people from hard-hit areas increased public attention to the outbreak and affected search behaviors [47,48]. Therefore, in addition to considering the impacts of actual pandemic severity on regional public attention, the impacts of socioeconomic conditions and population mobility should be simultaneously observed in order to accurately estimate the regional public risk perception.

To address the above research gaps, we investigated the regional public attention and regional public risk perception of the COVID-19 pandemic in China. We applied a multi-level spatiotemporal heterogeneous analytical framework using a series of spatiotemporal regressions based on Bayesian Spatiotemporally Varying Coefficients (STVC) modeling. Specifically, the STVC model is an emerging Bayesian local regression approach that is used for exploring the spatiotemporal heterogeneous/varying relationships between dependent and independent variables [49,50]. To further evaluate the spatiotemporal interaction effects of observable explanatory

variables on the target variable, we updated the STVC model with a new Spatiotemporally Interacting Varying Coefficients (STIVC) model. Our objective with China's case study is four-fold. Using Baidu Index, we first collected and processed internet search engine data to represent daily regional public attention to COVID-19 across 366 prefecture-level cities during the first nationwide pandemic wave. Then, we utilized Bayesian STVC series models, mainly including STVC and STIVC, to investigate the *in situ* spatiotemporal variations of the regional public attention regarding COVID-19 as well as the spatiotemporal heterogeneous associations between the regional public attention and the actual severity of COVID-19 at multiple administrative levels (i.e., national, provincial, and city levels) of China. Further, we put forward a regional public risk perception index (PRPI) as a more informative indicator to elucidate the collective human responses to COVID-19 within each city and across various stages in China. Finally, we produced maps of regional PRPI and identified their cluster and outlier areas to alert potential public sensitive areas in China.

## 2. Material and methods

### 2.1. Data

Internet search engine data can quantitatively depict the regional public attention in response to COVID-19, widely over a country, locally at sub-national scales, and spatiotemporally. The most widely used internet search product internationally is Google Trends [12,22]. However, Google withdrew from China in 2010, and Baidu (a Google equivalent) serves as China's most representative internet search product for exploring the public's online search behaviors. Based on Baidu's massive netizens' behavior data, Baidu Index (https://index.baidu.com/) can tell users how much a particular keyword (weighted search frequency) has been searched on Baidu, the trend of ups and downs over time, and where the netizens who pay attention to these keywords are geographically distributed [10]. Like Google Trends, Baidu Index can be restricted to a specific administrative location (e.g., city) and a specific period (e.g., day) to measure the real-time internet-derived public attention to COVID-19. Since 82.47% of Chinese internet users have been using the Baidu search engine to retrieve their information as of September 2021, this study adopted the Baidu Index to reflect daily public attention to COVID-19 across 366 prefecture-level cities in China for the first time [39,40].

We retrieved the original Baidu Index data through a publicly available tool (https://github.com/Hexmagic/BaiduIndexNew), which uses Python technologies to simulate users' operations on the Baidu Index web page and uses image recognition technologies to obtain the final Baidu index data corresponding to keywords at different times and in different regions in numerical forms [51]. Our city-level Baidu Index data covers the study period from December 31, 2019 (the first case of public reporting information in China) to March 18, 2020 (pandemic under control over China), which is recognized as China's first nationwide pandemic wave [3,4,52]. We selected twelve Baidu Index keywords regarding COVID-19 from those with the highest ranking in the search volume during the study period, as recommended by an official Baidu Keyword Mining platform (http://stool.chinaz.com) [51]. The twelve search keywords regarding COVID-19 are (in Chinese): "Pneumonia of unknown cause", "Real-time updates on the COVID-19 across the country", "Asymptomatic carrier", "COVID-19", "What are the symptoms of COVID-19", "The latest on COVID-19", "COVID-19 map", "COVID-19 (in English)", "2019-ncov", "sars", "ncp (novel coronavirus pneumonia)", and "SARS-CoV-2".

In general, the target variable, such as COVID-19 regional public attention, within regression-like modeling can only be one. However, more than one research keyword related to the phenomenon of interest can be obtained via Google Trends or Baidu Index. Here, we adopted the principal component analysis (PCA) to reduce the dimensionality of datasets and extract the most critical information as a one-dimension variable from twelve search keywords [53]. The PCA's first component (renamed as 'composite Baidu Index') represents the overall daily public attention to COVID-19 within each city throughout the study period in China, which is further used as the dependent variable in the following models (Supplementary Table 1).

Including daily reported disease cases, we also collected regional data on the daily population mobility status and yearly urban socioeconomic conditions that may influence the regional online public attention to COVID-19. The historical city-level reported data of COVID-19 in China, including daily cumulative cases and daily new cases, were obtained from an open-source COVID-19 data collection and analytics platform [54]. For the same period, we obtained the population mobility data, including inflow and outflow population, from the Baidu Migration platform (http://qianxi.baidu.com) to quantify the daily movement of the population across cities in China. We also collected twenty urban socioeconomic factors that may depict spatial disparities in searching behavior among multiple cities from the latest published China City Statistical Yearbook (http://www.stats.gov.cn/tjsj/). Due to raw data limitations, these city-specific socioeconomic covariates do not reflect daily variation characteristics. To reduce the multicollinearity issue by limiting the variance inflation factor (VIF) to less than 10, we selected GDP per capita, population density of primary industry employees, and average employee salary as final socioeconomic covariates from twenty variables [55]. Supplementary Table 2 summarizes the details of these urban socioeconomic covariates and their VIF values. These regional socioeconomic factors were only treated as auxiliary covariates to control the main effects of those space–time factors with daily variations. All geospatial-scale data used is publicly accessible and does not involve any personal information, so no ethical approval is required.

### 2.2. Statistical analytics

#### 2.2.1. Multi-level spatiotemporal heterogeneous modeling framework

We developed a generic framework of multi-level spatiotemporal heterogeneous modeling (Fig. 1) to investigate the COVID-19 pandemic by focusing on the regional public attention and regional public risk perception (associations between public attention and local pandemic risk levels). We regressed city-specific public attention to COVID-19 (Y) across 366 cities and throughout the pandemic wave of COVID-19 in China with the consideration of three aspects of explanatory factors (Xs) — local pandemic risks (X1 and X2) as the core factors, population mobility (X3 and X4) and urban socioeconomic conditions (X5-X7) as the control factors. To be specific, the seven explanatory factors were cumulative cases (X1), new cases (X2), inflow population (X3), outflow population (X4),

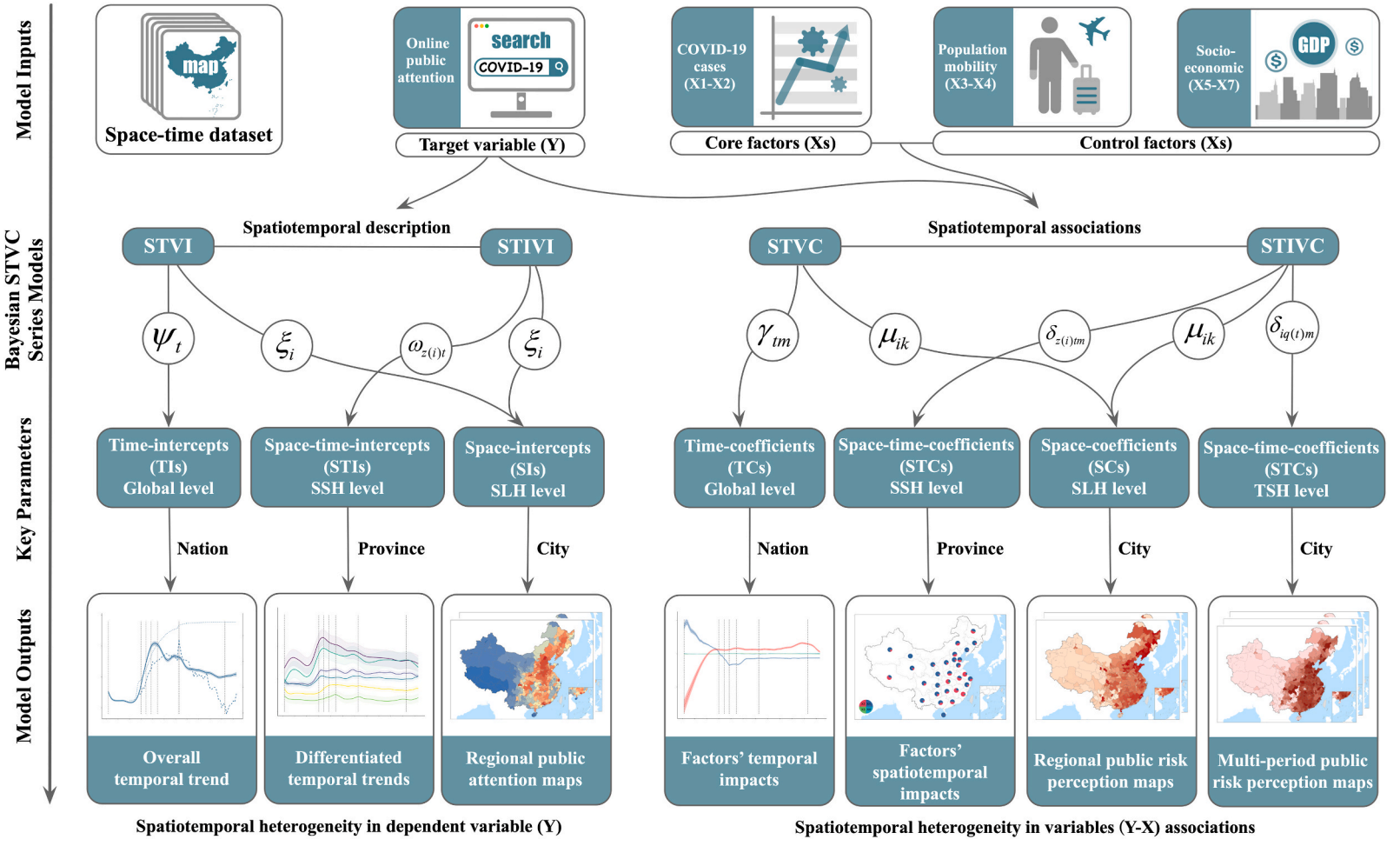


**Fig. 1.** Multi-level spatiotemporal heterogeneous modeling framework using Bayesian Spatiotemporally Varying Coefficients (STVC) series models. Variables: regional online public attention (Y), cumulative cases (X1), new cases (X2), inflow population (X3), outflow population (X4), GDP per capita (X5), population density of primary industry employees (X6), and average employee salary (X7). Only Y and X1 through X4 have both spatial and temporal variability. Bayesian STVC series models include two interpretive spatiotemporal regressions, Bayesian STVC and Spatiotemporally Interacting Varying Coefficients (STIVC) models, and two descriptive spatiotemporal regressions, Bayesian Spatiotemporally Varying Intercepts (STVI) and Spatiotemporally Interacting Varying Intercepts (STIVI) models. These four sub-models within the STVC series modeling system have different parameter interpretations and cannot be replaced by each other. SLH: spatial local heterogeneity, SSH: spatial stratified heterogeneity, TSH: temporal stratified heterogeneity.

GDP per capita (X5), population density of primary industry employees (X6), and average employee salary (X7). All factors were normalized to eliminate the dimensional impact and ensure their comparability within regression modeling.

Regarding China's COVID-19 research, we focused on two main objectives supported by this multi-level spatiotemporal analytical framework. The first objective of this study was to investigate how the regional public attention (composite Baidu Index) was spatiotemporally distributed at the national, provincial, and city levels throughout China with descriptive regressions. The second objective was to explore how the explanatory factors are associated spatiotemporally with the disparities in regional public attention using interpretative regressions. The city-specific associations between regional public attention (Y) and reported cases (X1 and X2) were further extracted for mapping the regional public risk perception across Chinese cities. These two objectives were achieved with the consideration of two underlying characteristics: spatiotemporal heterogeneity and multiple levels (e.g., national, provincial, and city levels in China).

The core and key statistical technology for implementing this analytical framework lies in the Bayesian STVC-based series models belonging to a generic class of spatiotemporal non-stationary regression. Based on the Bayesian STVC model, a full-map local regression to identify the spatiotemporal heterogeneity in relationships of variables [49,50], we propose a more sophisticated Bayesian STIVC model with the pivotal incorporation of the covariates' spatiotemporal interaction non-stationarity [56] based on the spatial stratified heterogeneity (SSH) [57] and the temporal stratified heterogeneity (TSH). Bayesian STVC and STIVC models are seen as interpretive tools (analysis for influence factors) for identifying spatiotemporal heterogeneous associations among variables [50,58]. We adopted the Spatiotemporally Varying Intercepts (STVI) and Spatiotemporally Interacting Varying Intercepts (STIVI) models, which are two simplified forms of the STVC and STIVC models without incorporating explanatory factors' spatiotemporal non-stationary effects. Unlike STVC and STIVC models, the STVI and STIVI models belong to those descriptive approaches (or space–time smoothed mapping methods) for describing the dependent variable (Y) [59,60].

Finally, we collected and visualized those critical space–time scale outputs from Bayesian STVC series models (STVI, STIVI, STVC, and STIVC) to help understand the phenomenon of interest. Bayesian STVI and STIVI models estimated three sets of posterior parameters for the dependent variable (Y), i.e., time-intercepts (TIs), space-intercepts (SIs), and space–time-intercepts (STIs), which referred to the overall temporal trend of public attention to COVID-19 at the national level, differentiated temporal trends at the provincial level, and spatial variations at the city level. In contrast, Bayesian STVC and STIVC models estimated time-coefficients (TCs), space-coefficients (SCs), and space–time-coefficients (STCs) as another three key posterior parameters to determine the associations of explanatory factors with public attention at the national, provincial, and city levels, among which the SCs and STCs of associations between regional public attention and local pandemic risk levels (X1 and X2) led to the final proposition of the regional public risk perception index (PRPI).

### 2.2.2. Bayesian STVC model

Spatiotemporally Varying Coefficients (STVC) model is a kind of Bayesian local spatiotemporal non-stationary regression, aiming to simultaneously quantify spatial and temporal heterogeneous associations between the dependent variable (Y) and various independent variables (Xs) with the consideration of spatial and temporal autocorrelation [49,50]. The Bayesian STVC model is designed to discover the structured spatiotemporal non-stationarity inherent in geospatial-related research questions. Compared with the frequentist-based local spatiotemporal non-stationary regressions [61,62], Bayesian ones have the advantages of being to a real full-map (complete and unified) modeling approach [63,64], incorporating prior knowledge and uncertainties (credible intervals on parameters) into modeling directly [65,66], as well as being much more flexible in model extensibility [50].

The STVC model follows a space–time independent assumption to assure the feasibility of Bayesian inference and computation, which is particularly convenient for spatiotemporal big data research with a larger range and a more refined scale [50]. Equations (1) and (2) give the complete form of an STVC model.

$$\eta_{it} = g(y_{it} \in Y) = \sum_{k=1}^{K} f_S(\mu_{ik} SX_{itk}) + \sum_{m=1}^{M} f_T(\gamma_{tm} TX_{itm}) + f_S(\xi_i) + f_T(\psi_t) + \sum_{h=1}^{H} \beta_h CX_{ith} + \alpha + \varepsilon_{it} \tag{1}$$

$$\mu \sim N_{iCAR}\left(0, \left[\tau_\mu R_s\right]^-\right),\ \gamma \sim N_{RW}\left(0, \left[\tau_\gamma R_t\right]^-\right),\ \xi \sim N_{iCAR}\left(0, \left[\tau_\xi R_s\right]^-\right),\ \psi \sim N_{RW}\left(0, \left[\tau_\psi R_t\right]^-\right) \tag{2}$$

In equation (1), $\eta_{it} = g(y_{it} \in Y)$ denotes the data likelihood level, with $\eta_{it}$ being the structural additive predictors, $y_{it}$ being space–time observations of the city-level public attention (Y) in space $i$ and time $t$, and $g(\cdot)$ being the likelihood function to link $\eta_{it}$ and $y_{it}$. The right-hand side of equation (1) denotes the space–time process level, where $\eta_{it}$ can account for different types of fixed and random effects in an additive way. For an STVC model, three types of effects for observable explanatory factors can be incorporated: the spatial non-stationary random effects $\sum_{k=1}^{K} f_S(\mu_{ik} SX_{itk})$ for $K$ space-dimension factors $SX$ (X1-X7) with spatial variations, the temporal nonstationary random effects $\sum_{m=1}^{M} f_T(\gamma_{tm} TX_{itm})$ for $M$ time-dimension factors $TX$ (X1-X4) with both spatial and temporal variations, and the global-scale stationary fixed effects $\sum_{h=1}^{H} \beta_h CX_{ith}$ for $H$ additional factors $CX$. $\varepsilon_{it}$ represent modeling residuals at spatiotemporal units, which can be modeled via a normal distribution, $\varepsilon_{it} \sim N(0, \sigma_\varepsilon^2)$.

Among the STVC's six posterior parameters $\{\mu_{ik}, \gamma_{tm}, \beta_h, \xi_i, \psi_t, \alpha\}$, $\mu_{ik}$ are defined as the space-coefficients (SCs) representing the spatially heterogeneous associations between regional public attention ($Y$) and factors $SX$ across all study locations, $\gamma_{tm}$ are the time-coefficients (TCs) that measure the temporally heterogeneous associations between $Y$ and factors $TX$ during each time frame, $\beta_h$ are the overall coefficients of control factors $CX$ (no such factors in this case), $\xi_i$ are the space-intercepts (SIs) representing the spatial pattern of $Y$, $\psi_t$ are the time-intercepts (TIs) representing the temporal trend of $Y$, and $\alpha$ is the global intercept. Note that only the local parameters SCs and TCs are two necessary components of an STVC model, while all the other four parameters, including SIs and TIs, are optional [50,58,67].

Functions $f_S(\cdot)$ and $f_T(\cdot)$ denote the spatial and temporal latent Gaussian models (LGMs) adopted to estimate the random effects for local parameters SCs and SIs, and TCs and TIs [68,69], as described in equation (2). In detail, according to the first and the second law of geography [70,71], the intrinsic conditional autoregressive (iCAR) prior model is used as a common spatial LGM to consider the spatial autocorrelation to fit the random effects of spatial heterogeneity [72]. We set $\mu \sim N_{iCAR}(0,[\tau_\mu R_s]^-)$ and $\xi \sim N_{iCAR}(0,[\tau_\xi R_s]^-)$ for space-scale parameters $\mu_i = (\mu_1,\ldots,\mu_n)'$ and $\xi_i = (\xi_1,\ldots,\xi_n)'$, where $\tau_\mu$ and $\tau_\xi$ are precision parameters, $R_s$ is a $n \times n$ spatial neighborhood matrix with diagonal elements equal to the number of neighbors of each city and non-diagonal elements $(R_s)_{ij} = -1$ if cities $i$ and $j$ are neighbors, and $(R_s)_{ij} = 0$ otherwise; the symbol $-$ denotes the Moore–Penrose generalized inverse of a matrix [59]. Here, two cities are considered as neighbors if they share a common border. In contrast, the random walk (RW) prior model is adopted as a typical temporal LGM to estimate the temporally heterogeneous random effect using an autocorrelated neighboring structure. We set $\gamma \sim N_{RW}(0,[\tau_\gamma R_t]^-)$ and $\psi \sim N_{RW}(0,[\tau_\psi R_t]^-)$ regarding time-scale parameters $\gamma_t = (\gamma_1,\ldots,\gamma_T)'$ and $\psi_t = (\psi_1,\ldots,\psi_T)'$, where $\tau_\gamma$ and $\tau_\psi$ are precision parameters, and $R_t$ is the $T \times T$ structure matrix of a RW [59].

Moreover, in order to perform a descriptive spatiotemporal analysis simply for regional public attention to COVID-19 (Y), we reduced the STVC model into a global-scale spatiotemporal regression, renamed Spatiotemporally Varying Intercepts (STVI) model, by removing all covariates' non-stationary components, i.e., $\sum_{k=1}^{K} f_S(\mu_{ik} SX_{itk})$ and $\sum_{m=1}^{M} f_T(\gamma_{tm} TX_{itm})$. Such descriptive STVI model is expressed in equation (3),

$$\eta_{it} = g(y_{it} \in Y) = \sum\nolimits_{l=1}^{L} \beta_l X_{itl} + f_S(\xi_i) + f_T(\psi_t) + \alpha + \varepsilon_{it} \tag{3}$$

where $\sum_{l=1}^{L} X = \sum_{k=1}^{K} SX \cup \sum_{m=1}^{M} TX \cup \sum_{h=1}^{H} CX$, with $X$ denoting $L$ explanatory factors with an overall coefficient $\beta_l$ under the global stationary assumption. The STVI model is advantageous in analyzing the *in situ* spatiotemporal structured variations ($y_{it}$) by directly visualizing local parameters $\xi_i$ and $\psi_t$.

### 2.2.3. Bayesian STIVC model

A potential limitation of the original Bayesian STVC modeling lies in its assumption of space–time independence. A space–time interaction assumption for covariates' nonstationarity at the spatial local heterogeneity (SLH) level has been proposed under frequentist statistics [61,62]. Unfortunately, such frequentist-based local spatiotemporal non-stationary regression is not a full-map modeling approach, the issue of which can be avoided with Bayesian statistics [63,64]. Even so, under Bayesian statistics, an SLH-level spatiotemporal interaction non-stationary assumption could be too complex and lead to an unusable local regression with far worse model performances and unacceptable computing time, especially when facing the fine-scale spatiotemporal big data in practice [50].

To ensure a moderate modeling complexity and inference feasibility for a Bayesian non-stationary regression of spatiotemporal interaction, we propose a Bayesian Spatiotemporally Interacting Varying Coefficients (STIVC) model to incorporate the non-stationary random effects of spatiotemporal interaction for covariates (explanatory factors) at the spatial stratified heterogeneity (SSH) level, instead of at the SLH level (the most refined spatial scale). Geographical SSH is ubiquitous in the real natural world and society, for example, climate zones, worldwide continents, and various administrative levels within a country or a region [57,73]. Hence, the STIVC model using SSH to define the spatiotemporal interaction is called the standard STIVC model. This study adopts the provincial level of China as the SSH effect, in which each province includes various cities.

*2.2.3.1. Standard STIVC (with SSH-type spatiotemporal interaction) model.* For the study area of China, we considered two administrative levels of spatial heterogeneity, including the provincial level and the city level. We defined the LSH layer as $n$ first-level cities, labeled as $i = 1, \ldots, n$. For each first-level city $i$, daily observations are available, which are marked by $t = 1, \ldots, T$. The LSH layer is nested within the SSH layer and is defined as $m$ second-level provinces, labeled as $z = 1, \ldots, Z$. The complete form of a standard STIVC model with the SSH-type spatiotemporal interaction is formulated using equations (4) and (5).

$$\eta_{it} = g(y_{it} \in Y) = \sum\nolimits_{k=1}^{K} f_S(\mu_{ik} SX_{itk}) + \sum\nolimits_{m=1}^{M} f_{ST}\left(\delta_{z(i)tm} TX_{itm}\right) + f_S(\xi_i) + f_{ST}\left(\omega_{z(i)t}\right) + \sum\nolimits_{h=1}^{H} \beta_h CX_{ith} + \alpha + \varepsilon_{it} \tag{4}$$

$$\mu \sim N_{iCAR}\left(0,\left[\tau_\mu R_s\right]^-\right),\ \delta \sim N_{st}(0,[\tau_\delta R_{st}]^-),\ \xi \sim N_{iCAR}\left(0,\left[\tau_\xi R_s\right]^-\right),\ \omega \sim N_{st}(0,[\tau_\omega R_{st}]^-) \tag{5}$$

In equation (4), $z(i)$ denotes that the first SLH-level city $i$ belongs to the second SSH-level province $z$. In terms of covariates' posterior coefficients $\{\mu_{ik}, \delta_{z(i)tm}, \beta_h\}$, $\mu_{ik}$ and $\beta_h$ are the same as in equation (1), which denote the city-specific spatial non-stationary impacts of main factors (X1-X7) and national stationary impacts of control factors (no such factors in this case), respectively. The space–time parameters $\delta_{z(i)tm}$ represent the SSH-level spatiotemporal interaction non-stationary impacts of main factors (X1-X4) with daily variations, reflecting that in each province $z$, the factors' temporal impacts are heterogeneous. In terms of those posterior intercept components $\{\alpha, \xi_i, \omega_{z(i)t}\}$, $\alpha$ and $\xi_i$ represent the global intercept and the city-level spatial intercepts, respectively. The space–time parameters $\omega_{z(i)t}$ are the SSH-level spatiotemporal interaction intercepts to depict the public attention variations $y_{it}$ at the provincial level [74]. Spatiotemporal residuals $\varepsilon_{it}$ follow $\varepsilon_{it} \sim N(0,\sigma_\varepsilon^2)$.

In equation (5), the same iCAR prior model is utilized as the spatial LGM to estimate those space-varying parameters $\mu_{ik}$ and $\xi_i$ at the first SLH level with cities $i = 1, \ldots, n$. The main improvement of an STIVC model lies in incorporating the space–time interaction random effects for covariates' coefficients $\delta_{z(i)tm}$ and intercepts $\omega_{z(i)t}$ at the second SSH level with provinces $z = 1, \ldots, Z$. This essential parameter $\delta = (\delta_{11},\ldots,\delta_{1T},\ldots,\delta_{Z1},\ldots,\delta_{ZT})'$ is named space–time-coefficients (STCs) and is estimated by adopting a sophisticated spatiotemporal interaction prior model $f_{ST}(\cdot)$, that is, $\delta \sim N_{st}(0,[\tau_\delta R_{st}]^-)$, where $\tau_\delta$ is a precision parameter and $R_{st}$ represents a

$ZT \times ZT$ matrix designed as an interaction of the corresponding spatial and temporal structure matrices. In this case, the component $R_{st}$ is defined as $R_{st} = I_z \otimes R_t$, where $\otimes$ denotes the Kronecker product, $I_z$ denotes an identity matrix of SSH dimension $Z \times Z$, following an exchangeable prior distribution that is given for the second provincial-level random effects, and $R_t$ denotes a $T \times T$ structure matrix of time following an RW prior model [56]. This type of space–time interaction assumes that the structured temporal trends are different from region to region at the SSH-based provincial level. In practice, we have four types of spatiotemporal interactions to choose from Ref. [56]. Similarly, the same $f_{ST}(\cdot)$ can be used to estimate the space–time-intercepts (STIs) $\omega = (\omega_{11}, ..., \omega_{1T}, ..., \omega_{Z1}, ..., \omega_{ZT})'$, that is, $\omega \sim N_{st}(0, [\tau_\omega R_{st}]^-)$. Like an STVC model, only the local parameters SCs ($\mu_{ik}$) and STCs ($\delta_{z(i)tm}$) are two indispensable components of an STIVC model, while all other posterior parameters are alternative.

After removing the explanatory factors' non-stationary random effects, i.e., $\sum_{k=1}^{K} f_S(\mu_{ik} SX_{itk})$ and $\sum_{m=1}^{M} f_{ST}(\delta_{z(i)tm} TX_{itm})$, the STIVC model is reformed into a Spatiotemporally Interacting Varying Intercepts (STIVI) model, as presented in equation (6). Compared with the previous STVI model, the STIVI model is more efficient in exploring the temporal variations of regional public attention $y_{it}$ in each province instead of over China as a whole by taking advantage of the space–time parameters STIs ($\omega_{z(i)t}$).

$$\eta_{it} = g(y_{it} \in Y) = \sum_{l=1}^{L} \beta_l X_{itl} + f_S(\xi_i) + f_{ST}(\omega_{z(i)t}) + \alpha + \varepsilon_{it} \tag{6}$$

*2.2.3.2. Extended STIVC (with TSH-type spatiotemporal interaction) model.* To ensure moderate model complexity, the standard STIVC model estimates the spatiotemporal interaction random effect by sacrificing the space scale, e.g., from city to province level of China. In practice, we could have geospatial data collected at many time points that can be divided into different stages (time intervals). Under this condition, we may want to keep the space scale constant and explore its varying patterns across various stages. To meet this requirement, instead of weakening the space scale based on SSH, we introduce the temporal stratified heterogeneity (TSH) to develop an extended variant of the Bayesian STIVC model by defining the spatiotemporal interaction random effect through grouping the time span, leading to the regression relationships of variables kept to the smallest space scale but with temporal disparities across various stages.

Here, we constructed a customized STIVC model for mapping China's varying public risk perception of COVID-19, without considering spatiotemporal intercept terms, global auxiliary explanatory variables, and the global intercept, which are not indispensable for an STIVC model. For each city $i$, daily observations marked by $t = 1, \ldots, T$ are available. Assuming that these temporal observations can be further divided into $Q$ stages (time intervals), labeled as $q = 1, \ldots, Q$, the customized STIVC model with TSH-type spatiotemporal interaction in line with China's COVID-19 case is formulated in equations (7) and (8).

$$\eta_{it} = g(y_{it} \in Y) = \sum_{m=1}^{M} f_{ST}(\delta_{iq(t)m} TX_{itm}) + \sum_{m=1}^{M} f_T(\gamma_{tm} TX_{itm}) + \sum_{d=1}^{D} f_S(\mu_{id} sx_{id}) + \varepsilon_{it} \tag{7}$$

$$\delta \sim N_{st}(0, [\tau_\delta R_{st}]^-),\ \gamma \sim N_{RW}(0, [\tau_\gamma R_t]^-),\ \mu \sim N_{iCAR}(0, [\tau_\mu R_s]^-) \tag{8}$$

In equations (7) and (8), $q(t)$ denotes that the daily observation $t$ belongs to the upper temporal stage $q$. The model estimates three categories of posterior coefficients, i.e., $\{\delta_{iq(t)m}, \gamma_{tm}, \mu_{id}\}$. For $M$ explanatory factors $TX_{itm}$ (X1-X4) with both space and time variations, the STCs ($\delta_{iq(t)m}$) is estimated at the city level and across various periods, and the TCs ($\gamma_{tm}$) is estimated at the overall national level. As for $D$ spatial covariates $sx_{id}$ (X5-X7) without daily variations, the SCs ($\mu_{id}$) is estimated at the city level. The prior LGMs $f(\cdot)$ for parameters TCs and SCs are the same as defined in equations (1)–(4). Here, the space–time interaction component $R_{st}$ is defined as $R_{st} = R_i \otimes I_q$, where $\otimes$ denotes the Kronecker product, $R_i$ denotes a $n \times n$ spatial structure matrix following an iCAR prior model, and $I_q$ denotes an identity matrix $Q \times Q$ following an exchangeable prior distribution that is given for the temporal stratified random effect [56,59]. This type of space–time interaction assumes that the structured spatial patterns are different from time to time at the TSH level. The local parameters STCs $\delta = (\delta_{11}, ..., \delta_{1Q}, ..., \delta_{n1}, ..., \delta_{nQ})'$ describe the time-varying spatial associations between Y and space–time factors. This case study only used the extended STIVC (TSH-type) model to estimate STCs ($\delta_{iq(t)m}$) to reveal the temporal dynamics of spatial public risk perception maps of COVID-19 across Chinese cities. The reduced intercept-version of this extended STIVC (TSH-type) model is not shown here but can be implemented in a similar way to formulas (3) and (6).

### 2.2.4. Bayesian random-effect contribution percentage index

Beyond establishing Bayesian STVC series models, we simultaneously obtained a Bayesian random-effect contribution percentage (RCP) index and its 95% credible intervals (CIs) to qualify the relative contribution (%) of one or more random effect components (e.g., spatial and temporal LGMs) in total variations of the target variable using the posterior variances of hyperparameters (details in Supplementary Note 3). The Bayesian RCP index is used to provide quantitative information (percentage) on how much different components (e.g., temporal, spatial, and spatiotemporal interaction random effects) can explain the space–time variations of China's city-level public attention to COVID-19, as well as to identify the overall contribution of explanatory factors after considering their spatiotemporal heterogeneous associations with the target variable. Compared to mainstream methods in identifying the factors' relative importance [57,75], the advantages of such an STVC-based RCP index mainly lie in two aspects. On the one hand, instead of detecting the factors' relative importance under a stationary assumption, the RCP index can characterize these considering their spatiotemporal nonstationarity supported by Bayesian STVC series models. On the other hand, the 95% Bayesian CIs of the RCP index can be simultaneously contained to access evaluation uncertainties via modern Bayesian computing methods and tools [66].

### 2.3. Inference, implementation, and evaluation for Bayesian STVC series models

We employed the integrated nested Laplace approximation (INLA), a computational-efficient Bayesian inference method to estimate the posterior parameters of the Bayesian STVC series models and calculate the Bayesian RCP index in software R through the R-INLA package [69,76]. For this case study, log-gaussian was set as the likelihood function in R-INLA. The prior LGMs for fitting the spatial and temporal random effects of local regression parameters were set as iCAR and RW models, respectively, with hyper-parameters set as Penalized Complexity (PC) priors on the standard deviation. Consistent with common PC priors, we specified that the probability of the standard deviation being greater than 1 is small, equal to 0.01 [65,66]. The key posterior parameters estimated by Bayesian STVC series models mainly included SCs, TCs, and STCs, which are jointly utilized to reveal the complex, multi-level, and heterogeneous relationships among variables under the space–time dimension. We used samples of 100,000 times for the RCP index to obtain its 95% Bayesian CIs.

We summarized the specific formulas of the implemented Bayesian STVC family of models (Supplementary Note 4), including STVI, STIVI, STVC, STIVC (SSH-type), and STIVC (TSH-type), and evaluated their modeling performances (Supplementary Table 3). The STIVC models turned out to be the optimal regressions with the best model fitness and predictability, revealing the effectiveness of constructing spatiotemporal interaction random effects for observable explanatory factors combined with SSH/TSH theories. Among two STIVC models, the standard STIVC (SSH-type) model is more practical because it identifies the day-by-day temporal heterogeneity within each province, which is of great significance for regional-specific time-varying pandemic prevention and control. In contrast, the extended STIVC (TSH-type) model sacrifices the time precision and is only used as a complement for producing multi-period public risk perception maps. It should also be noted that five sub-models within the Bayesian STVC series modeling system cannot be substituted for each other because their key posterior parameters are different in the interpretation of practical applications. For instance, only the STVC model could estimate the average spatial effect over the study area for producing the total public risk perception map; and only the standard STIVC (SSH-type) model was appropriate for detecting fine-scale time differences within each region, consistent with our research focusing on daily risks of COVID-19. The applied scenarios of the five Bayesian STVC-based models are shown and compared in the results section.

### 2.4. Regional public risk perception index and mapping

We propose a regional index about public risk perception, representing the spatial heterogeneous/varying associations between the regional public attention and the actual risk of local emergencies, using Bayesian STVC and STIVC models. Here, the regional public risk perception index (PRPI) for China's COVID-19 public attention case is calculated using equations (9) and (10).

$$PRPI_i = \mu_{i,X1} + \mu_{i,X2} \text{ for STVC and STIVC (SSH-type) models} \tag{9}$$

$$PRPI_{iq_{(t)}} = \delta_{iq(t),X1} + \delta_{iq(t),X2} \text{ for the STIVC (TSH-type) model} \tag{10}$$

The local parameter $\mu_i$ denotes the posterior median values of SCs in each city $i$, estimated by the STVC or the standard STIVC (SSH-type) model. Covariates X1 and X2 are cumulative cases and new cases of COVID-19, jointly representing the city-specific severity of the COVID-19 pandemic. The $\mu_i$ from the STVC model depicts the average spatial effect of PRPI. In contrast, the $\mu_i$ from the standard STIVC (SSH-type) model should be seen as a residual or excess spatial effect of PRPI as its estimation removes the second provincial-level spatiotemporal interaction effects. The local parameter $\delta_{iq(t)}$ from the STIVC (TSH-type) model denotes the posterior median values of STCs for each city $i$ and each time interval $q(t)$, referring to the time-varying regional patterns of PRPI. Concerning other studies, one or more different factors should be selected to represent the actual local risk of a major emergency.

To detect public sensitive areas, we adopted a mainstream cluster and outlier analysis approach for regional PRPI maps to detect their statistically significant hot spots, cold spots, and two types of spatial outliers based on the Anselin Local Moran's I statistic in ArcGIS software [77]. Four types of informative zones about COVID-19 regional risk perception were identified: High-High Cluster with high public attention and severe outbreaks of COVID-19, High-Low Outlier with high public attention but mild outbreaks, Low-High Outlier with low public attention but severe outbreaks, and Low-Low Cluster with low public attention and mild outbreaks. The Not Significant areas in cluster and outlier maps indicate that the regional PRPIs among these cities are not statistically significant (less than 90% confidence) to form a cluster or an outlier.

## 3. Results

### 3.1. Spatiotemporal disparities in regional public attention to COVID-19 in China

Using the Bayesian STVI and STIVI models, we first analyzed the temporal trends of daily public attention to COVID-19 at national and provincial levels during the pandemic wave in China so far. We focused on seven key events (events I-VII) within the period from December 31, 2019, when the Wuhan Health Commission announced a possible outbreak of an unknown new pneumonia, to March 18, 2020, one week after the World Health Organization (WHO) declared a pandemic and local pandemic was under control throughout China (Fig. 2a) [3,21]. After the Wuhan Health Commission announcement (event I), national-level public attention remained steady at the outset and increased rapidly after two weeks when human-to-human transmission of an unknown new pneumonia was confirmed (event II). During this period, national-level public attention followed a similar pattern of daily reported cases and continued to increase for the next four days when the Wuhan city lockdown was announced (event III) and peaked two days later when public health emergency responses were activated in all provinces across China (event IV). National public attention decreased steadily but remained relatively higher than within the first two weeks, despite the WHO declaring COVID-19 to be a public

health emergency of international concern (event V), which was followed by news of mass infections in prisons in China (event VI), and the declaration of a pandemic by the WHO three months after the initial announcement of an outbreak (event VII) (Fig. 2b). This could be attributed to the decreased number of new cases identified in China as well as the steady number of cumulative cases reported during the corresponding period (Fig. 2b).

While changes in the overall national public attention correlated to key events taking place in China, at the provincial level, large disparities were observed in different regions and provincial-level trends were found to deviate from the national public attention trend (Fig. 2c and Supplementary Fig. 1). Unlike the national-level public attention, there was a relatively more immediate increase in public attention in the provincial level cities of Beijing and Shanghai, which decreased before the decrease in the national trend (events II to VII). In contrast, public attention in some provinces, such as Hubei (the province where Wuhan city is located), Guangdong, Xinjiang, and Tibet, trended much lower during the same period (between events I and II). In some of these provinces, public attention peaked later than in Beijing or Shanghai, and subsequent temporal fluctuations failed to follow the national trend (events II to VII) (Fig. 2c).

The temporal differences identified at the provincial level suggested the existence of substantial regional disparities in the public attention to COVID-19 across China. To further investigate if there were city-specific differences in public attention, we first used the

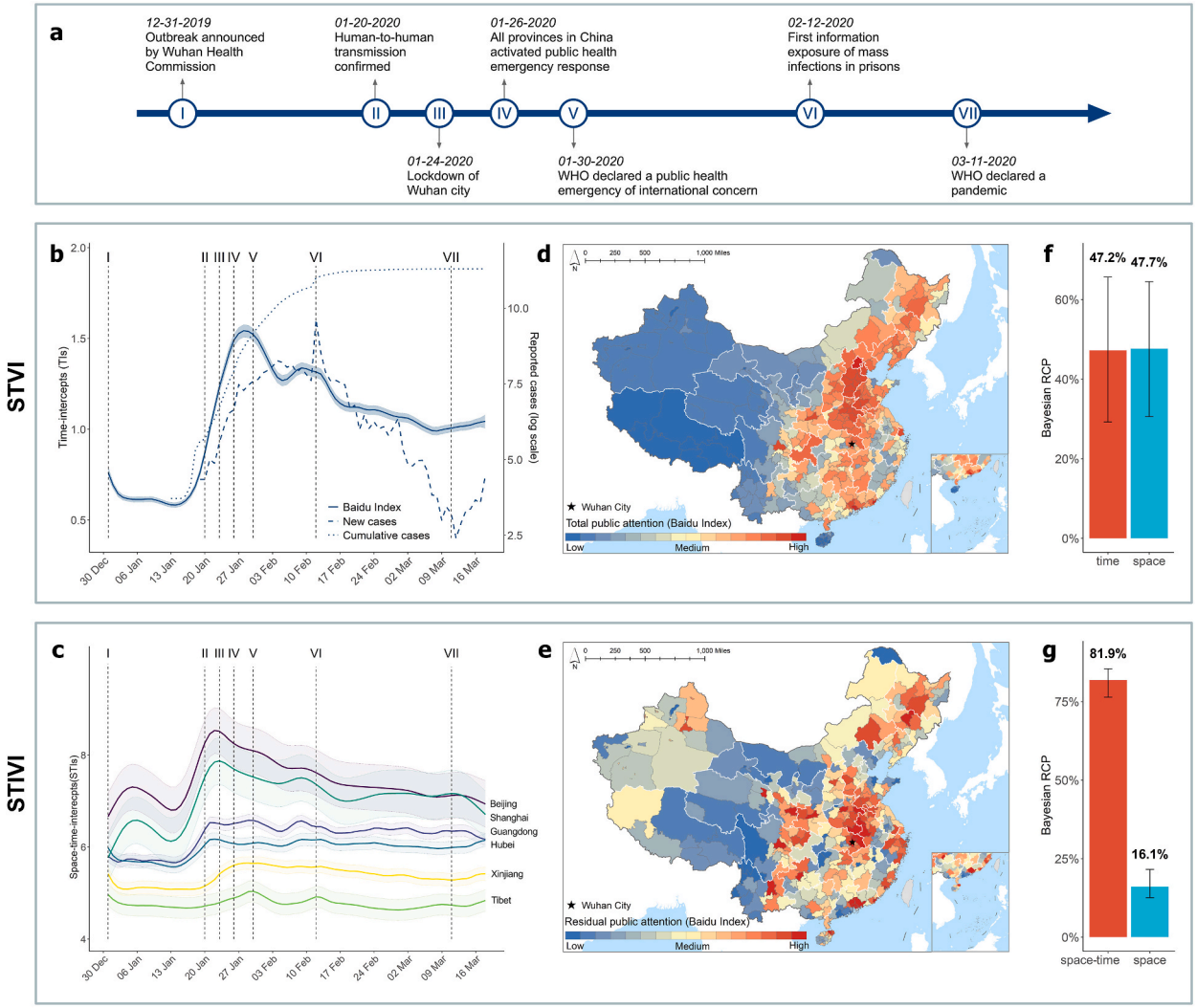


**Fig. 2.** Temporal and spatial disparities in regional public attention (Baidu Index) to COVID-19 between China's national, provincial, and city levels. a, Timeline of seven key COVID-19 events (I-VII) during China's first pandemic wave from December 31, 2019 to March 18, 2020. b, The overall time trend of the national public attention using parameter time-intercepts (TIs) with 95% CIs; c, Spatial disparities in six representative provincial-level time trends of public attention using parameter space–time-intercepts (STIs) with 95% CIs; d, Total public attention map to present regular regional patterns among cities using parameter space-intercepts (SIs). e, Residual public attention map to identify irregular regional differences among cities using parameter SIs by adjusting the provincial-level spatiotemporal interactive effects. f, Percentages (Bayesian RCP index with 95% CIs) of public attention variations explained by the national-level temporal trend (b) and the total city-level spatial patterns (d). g, Percentages of public attention variations explained by the provincial-level temporal trends (c) and the residual city-specific spatial differences (e). Panels b, d, f are extracted from the STVI model, and panels c, e, g are extracted from the standard STIVI model.

Bayesian STVI model to generate the total public attention map across 366 cities (Fig. 2d). This map showed regional differences of clusters across China with higher public attention in the eastern provinces and lower public attention in the western provinces. In contrast, after using the Bayesian STIVI model to adjust for provincial-level spatiotemporal interactive variations (Fig. 2c), a residual public attention map was generated to reveal the irregular local differences between cities (Fig. 2e). By removing the provincial level impacts from the total public attention map, the residual map uncovered high attention cities in the lower public attention divisions such as Western China, and uncovered low attention cities in higher public attention divisions, such as Eastern, Southern, and Central China. For example, in the western province of Xinjiang, the total map suggested that the public attention in the whole province was low (Fig. 2d). However, the residual map suggested that public attention was not homogenous. While most parts of the province displayed a low to a medium pattern of public attention, public attention in the provincial capital, Ürümqi, was exceptionally high, comparable to major cities in the eastern provinces (Fig. 2e). This phenomenon was found to be similar in Qinghai province, where the total map suggested low public attention throughout the province, while the residual map indicated high public attention in the provincial capital of Xining. In practice, these two types of COVID-19 city-specific public attention maps can be applied to reveal regional clusters and local disparities, respectively.

We further calculated the Bayesian RCP index for STVI and STIVI models to quantify the degree to which variations in China's COVID-19 public attention could be explained by the temporal and spatial effects at various administrative levels. Given the regional public attention itself in the STVI model (Fig. 2f), we noticed that the national-level temporal trend (Fig. 2b) accounted for 47.2% (CIs: 9.2%–65.7%) of variations, while the remaining variations (47.7%, CIs: 30.6%–64.5%) were mainly contributed by the total city-level spatial patterns (Fig. 2d). Moreover, in the STIVI model (Fig. 2g), the provincial-differentiated trends (Fig. 2c) drastically increased the contribution of temporal dimension up to 81.9% (CIs: 76.4%–85.4%), resulting in the remaining city-specific spatial variations (16.1%, CIs: 12.6%–21.5%) being interpreted as the residual regional public attention (Fig. 2e). Lower uncertainties (narrower range of CIs) of spatiotemporal components in the STIVC model also suggest the necessity of incorporating the temporal effects of provincial-level differences for public attention instead of a single national-level temporal effect.

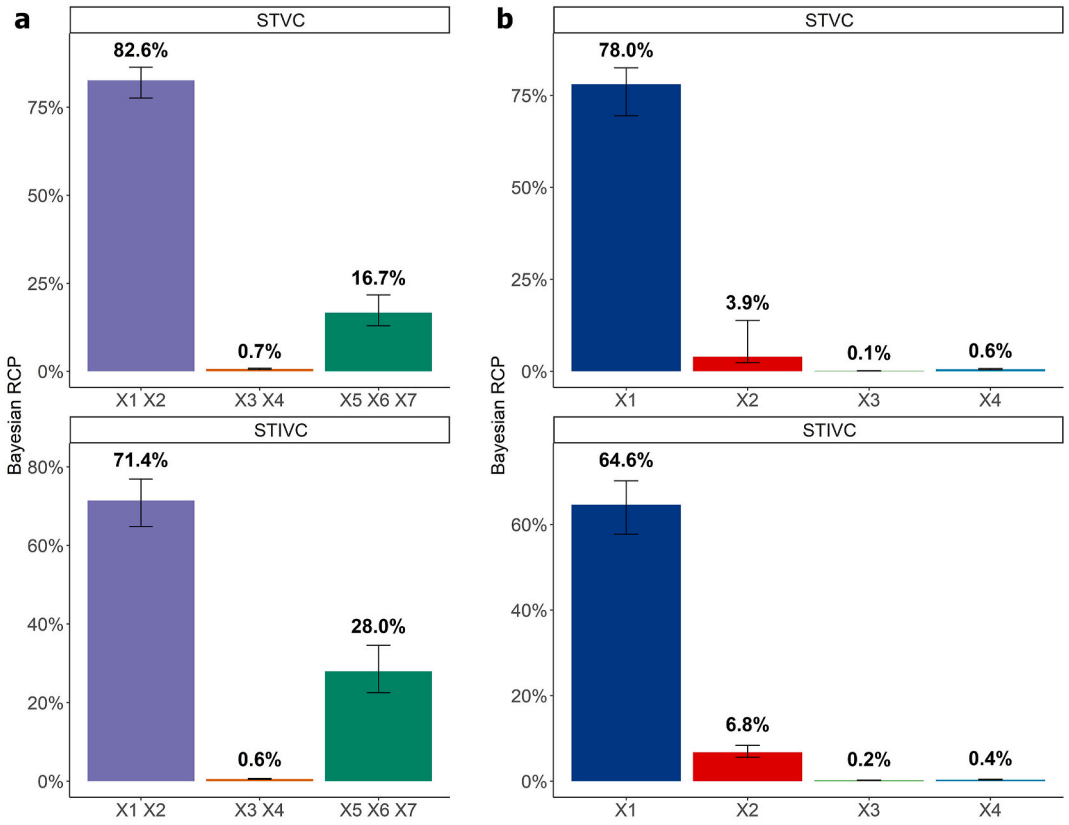


**Fig. 3.** Contribution percentages of factors accounting for spatiotemporal variations of China's city-level public attention to COVID-19. a, Contribution percentages (Bayesian RCP index with 95% CIs) of three main groups (I-III) of factors in STVC and standard STIVC models. Group I: daily COVID-19 cases (X1 cumulative cases, X2 new cases), group II: daily population mobility (X3 inflow population, X4 outflow population), and group III: urban socioeconomic conditions (X5 GDP per capita, X6 population density of primary industry employees, and X7 average employee salary). b, Contribution percentages of four daily varying factors (X1-X4) with both space and time variations in STVC and standard STIVC models. Here, the STIVC model refers to the standard model that takes the SSH-type spatiotemporal interactions into account.

### 3.2. Investigating factors affecting regional public attention to COVID-19

We have shown that regional public attention in China to the pandemic was not uniform and showed substantial disparities between national, provincial, and city levels (Fig. 2). Beyond descriptive modeling and mapping, elucidating the locally spatiotemporally varying relationships between COVID-19 regional public attention and potential influencing factors can lead to a better understanding of the collective human behavior during the COVID-19 pandemic. We further used the STVC and the standard STIVC (SSH-type) models to investigate the multi-level associations between regional public attention and seven city-specific factors (X1-X9) (Fig. 1). These seven factors covered three categories, i.e., group I: daily progression of COVID-19 (X1 cumulative cases, X2 new cases), group II: daily population mobility (X3 inflow population, X4 outflow population), and group III: urban socioeconomic conditions (X5 GDP per capita, X6 population density of primary industry employees, and X7 average employee salary). X1-X4 represented primary factors with both space and time variations. X5-X7 showed the urban socioeconomic differences in affecting original public web search behaviors. As urban socioeconomic factors were not published with daily variations, they were regarded as additional ancillary information and only served as space-scale control covariates in our models.

According to the Bayesian RCP evaluation results for STVC and standard STIVC (SSH-type) models (Fig. 3), we first found that the daily progression of COVID-19 (group I) accounted for most space–time variations of regional public attention, that is, 71.4% (CIs: 64.8%–76.9%) and 82.6% (CIs: 77.6%−86.4%), followed by the unban socioeconomic conditions (group III) with RCPs of 28.0% (CIs: 22.5%–34.6%) and 16.7% (CIs: 12.9%–21.7%) (Fig. 3a). In contrast, the daily population mobility status (group II) showed limited

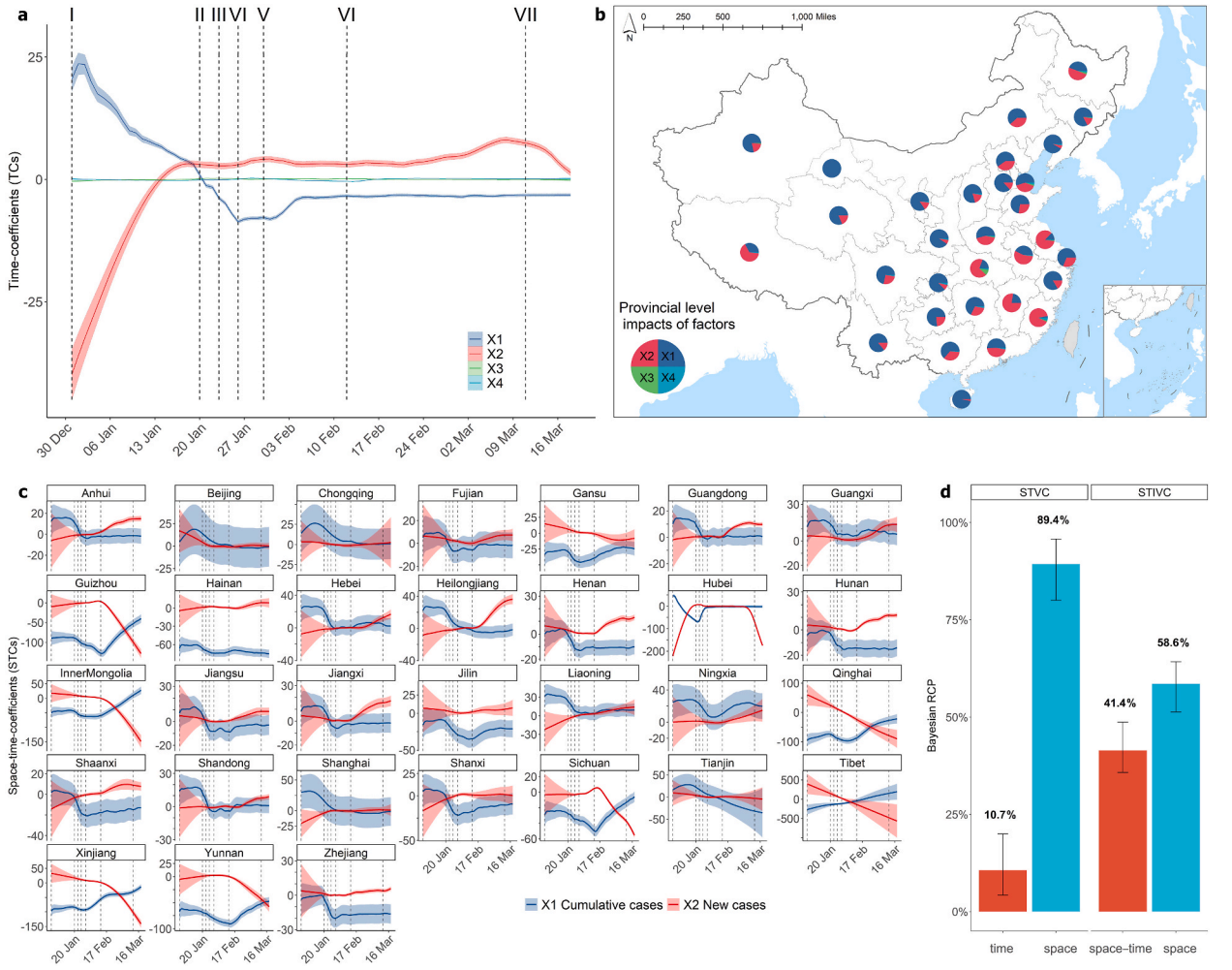


**Fig. 4.** Temporal heterogeneous associations between regional public attention and daily varying factors at the national and provincial levels in China. a, National-level impacts of daily varying factors (X1-X4) on public attention using parameter time-coefficients (TCs) with 95% CIs. b, Provincial-level average impacts of factors (X1-X4) on public attention mapped using the average effect of space–time-coefficients (STCs). c, Provincial-level public risk perception: temporally varying associations (STCs with 95% CIs) between daily public attention and COVID-19 cases (X1 and X2) demonstrated large disparities across 31 provinces in China. d, Bayesian RCP index with 95% CIs in STVC and STIVC models: differences in contribution percentages of factors at the time (national), space–time (provincial level) and space (city level) scales. Only factors X1 through X4 have time-dimension variations, namely, X1 cumulative cases, X2 new cases, X3 inflow population, and X4 outflow population. Vertical dashed lines represent those important events (I-VII) regarding China's COVID-19 development in terms of influencing collective public attention (Fig. 2a). Here, the STIVC model refers to the standard model with an SSH-type spatiotemporal interaction.

contribution to modeling regional public attention (0.6% with CIs 0.5%–0.7% and 0.7% with CIs 0.5%–0.9%) in both spatiotemporal models. Daily COVID-19 reported cases (X1 and X2) turned out to be the key driver of COVID-19 regional public attention in China. Regarding the four factors (X1-X4) with spatiotemporal variations (Fig. 3b), we further found that the daily cumulative cases (X1) with 64.6% (CIs: 57.7%–70.2%) and 78.0% (CIs: 69.5%–82.5%) accounted for much higher variations than the daily new cases (X2) with 6.8% (CIs: 5.6%–8.4%) and 3.9% (CIs: 2.3%–13.7%) in the STVC and STIVC (SSH-type) models. During the first wave in China, the daily mobility of citizens played a mild role (0.6%–0.7%) in affecting the spatiotemporal changes in urban public attention. To summarize, the spatiotemporal disparities in city-level collective public attention to COVID-19 were highly associated with daily reported cumulative and new cases.

### 3.3. Temporal associations between regional public attention and daily varying factors

Temporally, among four factors (X1-X4) with daily variations, we first found that the national-level influence of cumulative cases (X1) was much stronger than that of new cases (X2) at the beginning of the study period (Fig. 4a). In contrast, in the middle and later stages of the study period, new cases (X2) had more influence on public attention than cumulative cases (X1). Reflecting from the transition in major influence from cumulative cases to new cases, the change in public health policy in China after January 20, 2020, when the human-to-human transmission was confirmed (event II), might have played a key role in such alteration. After the WHO declared a public health emergency of international concern (event V), the impacts of cumulative cases (X1) stayed flat, which might be associated with the relatively slow increase in COVID-19 cumulative cases in China [52]. In contrast, the country-level impact of new cases (X2) increased rapidly and became stable after the lockdown in Wuhan (event III). In March 2020, China's pandemic was generally under control, and the daily reported new cases were less than ten [52]. As a result, the impacts of new cases (X2) showed a slightly decreasing trend since early March 2020. The results also showed that the national temporal contributions of inflow and outflow population (X3 and X4) were relatively small. The main factors that explained the national-level dynamics of public attention were the daily reported COVID-19 cumulative and new cases (X1 and X2).

At the provincial level, we introduced the STCs, critical outputs from the standard STIVC (SSH-type) model, to explore the spatiotemporal interactive associations between main space–time factors (X1-X4) and regional public attention. Consistent with national-level results (Figs. 3 and 4a), the provincial-differentiated contributions of both inflow (X3) and outflow (X4) population to public attention were found to be low in all provinces, whereas cumulative cases (X1) and new cases (X2) were highly correlated with regional public attention (Fig. 4b). We further evaluated the daily influences of cumulative and new cases on public attention in 31 provinces across China (Fig. 4c) and the daily influences of population mobility (Supplementary Fig. 2). These provincial associations between COVID-19 progression and regional public attention can also be interpreted as the provincial-level public risk perception of COVID-19. The daily influences of cumulative cases (X1) in most provinces were relatively consistent with those at the national level. However, the provincial-level public risk perception to cumulative cases of COVID-19 in nine provinces, such as Shaanxi, Inner Mongolia, and Tibet, showed an opposite trend compared to the national average. For new cases (X2) in most provinces, the daily varying impacts in most provinces on public attention increased first (after event II) and flattened afterward, which was generally consistent with the results at the national level. However, the public risk perception of new cases of COVID-19 in Qinghai, Tibet, Xinjiang, and other eight provinces demonstrated decreasing trends, especially in the middle (events II-VI) and late-stage (events VI-

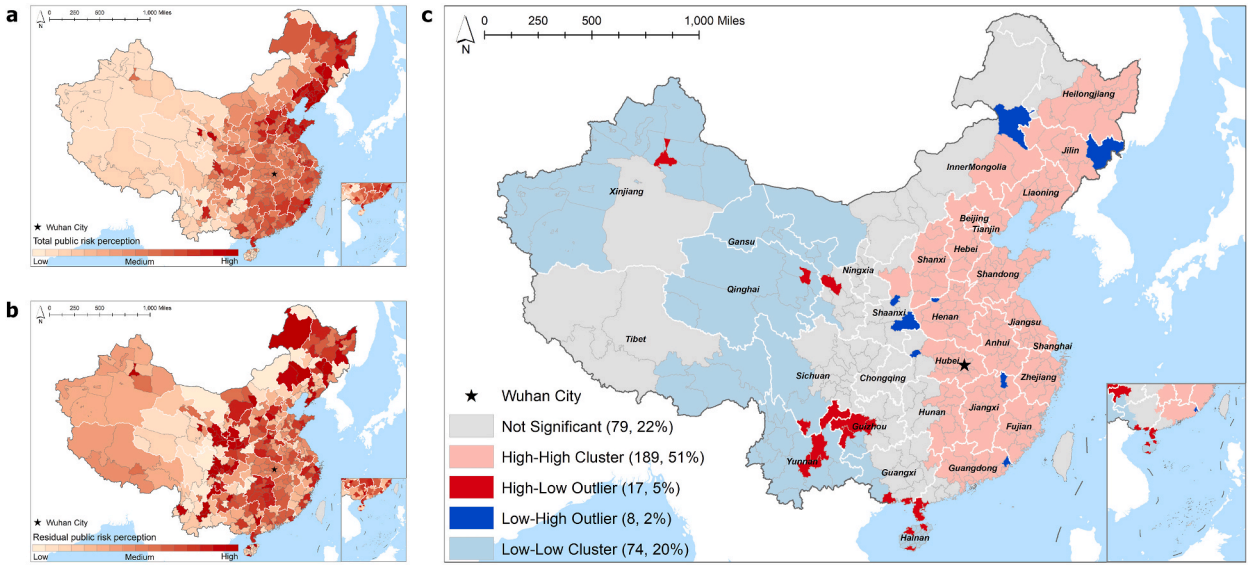


**Fig. 5.** Regional public risk perception of COVID-19 maps across Chinese cities. a, Total public risk perception map ($PRPI_i$ estimated by the STVC model) shows regular spatial differences and regional clusters. b, Residual public risk perception map ($PRPI_i$ estimated by the standard STIVC model) reveals the extra and irregular spatial differences among cities by removing the provincial spatiotemporal interactive effects. c, Cluster and outlier map of total public risk perception shows a more macroscopic pattern by detecting four types of statistically significant zone, namely, High-High Cluster, High-Low Outlier, Low-High Outlier, and Low-Low Cluster.

VII) of China's first wave. We further observed that during the worst pandemic phase (events V-VII), only the public in Beijing, Shanghai, Liaoning, and Hubei paid the same high-level attention to both new and cumulative cases, suggesting a uniform public risk perception in these four provincial-level regions.

Using Bayesian RCP indices, previous space–time decomposition in regional public attention (Fig. 2g) showed that the provincial-level temporal variations contributed more than the city-level spatial variations. However, after introducing spatiotemporal heterogeneous impacts of various factors on regional public attention (Fig. 4d), we discovered that the city-level impacts of factors were the most important, as they accounted for 89.4% (CIs: 80.2%–95.8%) of all contributions after adjusting the national-level temporal impacts (10.7%, CIs: 4.2%–19.8%) in the STVC model, and still accounted for 58.6% (CIs: 51.3%–64.2%) of all contributions after

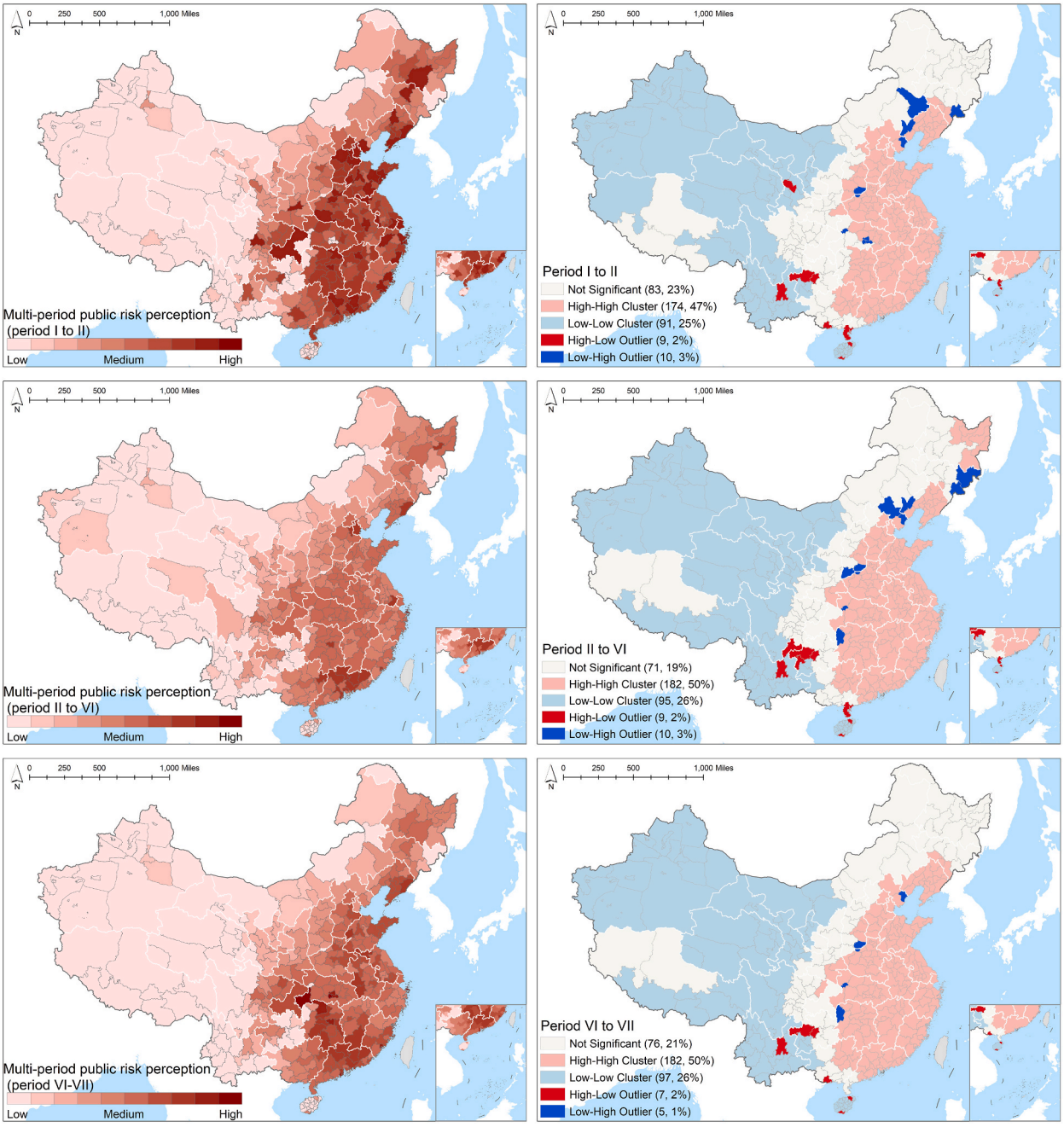


**Fig. 6.** Maps of multi-period regional public risk perception of COVID-19 considering the temporal stratified disparities (periods I to II, II to VI, and VI-VII) across Chinese cities, and their outlier and cluster maps. I-VII refer to key events related to COVID-19 progression during the nationwide wave in China (Fig. 2a). Three maps ($PRPI_{iq_{(t)}}$) use the same posterior space–time-coefficients (STCs) fitted by the extended Bayesian STIVC model with the TSH-type spatiotemporal interaction. A uniform standard is adopted for the color stratification of mapping.

adjusting the provincial differentiated temporal impacts (41.4%, CIs: 35.8%–48.7%) in the STIVC (SSH-type) model. Hence, mapping spatially heterogeneous associations between the local progression of COVID-19 (dominant factors) and regional public attention can aid in further determining the city-level public risk perception of COVID-19 in China.

### 3.4. Mapping regional public risk perception of COVID-19

The spatial associations between the progression of COVID-19 (daily cumulative and new cases) and regional public attention to it enabled us to further determine the regional public risk perception index (PRPI) at the city level during the pandemic in China. We first visualized three thematic maps of regional PRPI to describe collective internet human behaviors in response to COVID-19 across Chinese cities in general. Specifically, the total public risk perception map (Fig. 5a) was the sum of province-level trends and city-specific characteristics to show an overall pattern of risk perception, using $PRPI_i$ from the STVC model. The residual public risk perception map (Fig. 5b) removed the province-level spatiotemporal interactive effects and retained the city-specific additional risk perception, using $PRPI_i$ from the standard STIVC (SSH-type) model. The cluster and outlier map for total public risk perception (Fig. 5c) highlighted four categories of geographical zones concerning COVID-19 risk perception, i.e., clusters with high-attention to COVID-19 and high-risk of COVID-19 (High-High Cluster), clusters with low-attention and low-risk (Low-Low Cluster), outliers with high-attention but high-risk (High-Low Outlier), and outliers with low-attention and high-risk (Low-High Outlier).

Across 366 Chinese cities, the total public risk perception map (Fig. 5a) revealed obvious spatial gradient changes. In Central, South, and Northeast China, the COVID-19 cases were more influential on city-level public attention, while in West China, the city-level impacts of COVID-19 cases were at relatively low levels. Using its cluster and outlier map (Fig. 5c), we further showed that 189 (51%) cities were areas with high-risk and high-attention clusters, mainly distributed in Central, South, and Northeast China. High-High Cluster could refer to those normal response cities where the public maintained a high level of concern and the local infections were relatively severe. In contrast, 74 cities (20%) in West China were identified as low-risk and low-attention clusters, which could refer to those cities where the pandemic was relatively mild, and the public was relatively calm or unconcerned. Additionally, 8 cities (2%) were identified as outliers of low-attention but high-risk of COVID-19, suggesting that in these cities, although the pandemic was severe, the public's COVID-19 risk perception was relatively low. The public literacy in these cities might be relatively low, making guiding coordinated population actions essential for establishing local public health strategies. Lastly, 17 cities (5%) cities were identified as the high-attention but low-risk outliers, suggesting there could be an overabundance of attention compared with the severity of the pandemic in these cities. The city-level total public risk perception map and its cluster and outlier map were made to uncover spatial agglomeration areas where regional or clustered level strategies could be implemented. Throughout the entire study period, less than 10% of cities were recognized as outlier clusters. On the other hand, the residual public risk perception map (Fig. 5b) highlighted the irregular and additional city-specific risk perception after removing the provincial-level spatiotemporal interaction effects to further indicate whether one city would need more location-specific interventions. In practice, maps Fig. 5a and c might be helpful for rapid macro policy formulation targeting national, district, or regional organizations. In contrast, map Fig. 5b might be more helpful for local departments within a region in identifying areas that require additional attention.

The city-level associations between regional public attention and reported cases of infections could vary over time in practice, suggesting that the regional PRPI could also vary temporally. According to Fig. 2a and b, we delineated China's first round of COVID-19 (from December 31, 2019 to March 18, 2020) as three periods: the early state with low public attention (period I to II), the rapid rising stage of public attention (period II to VI), and the leveling-off stage of public attention (period VI-VII). Our primary consideration for choosing event II (when the human-to-human transmission was confirmed) and event VI (news of mass infections in prisons in China) as the time separation points lies in that, since event II, the national public attention in China rose rapidly and peaked in about one week. Event VI was the last major event to raise public attention in China, after which, public attention continued to decline but remained relatively high. Considering the above three stages of public attention in the progression of China's COVID-19 pandemic, we finally produced the multi-period regional public risk perception maps (Fig. 6), using the $PRPI_{iq_{(t)}}$ (posterior STCs) estimated by the extended STIVC (TSH-type) model. The overall spatial patterns of regional PRPI of the three stages were found to be similar, but the risk perception of the early stage (I-II) was the highest. As China's pandemic progressed onto a relatively stable stage, the percentage of abnormal cities with high-low and low-high outliers declined from 5% in the first (I-II) and second (II to VI) periods to 3% in the third period (VI-VII). Time-varying regional public risk perception maps are expected to assist dynamic change in policymaking of the real-time prevention and control of the ongoing COVID-19 pandemic.

## 4. Discussion

While collective human attention is indispensable to pandemic control and prevention, regional public attention in response to the COVID-19 pandemic was not taken seriously or utilized effectively worldwide [9,10,12]. This is the first in-depth study, to our knowledge, investigating regional public attention and regional public risk perception of COVID-19 using city-level internet search engine data in China. We came up with an innovative regional index (PRPI) to depict the spatial heterogeneous associations between regional public attention and actual local severity of a major emergency, e.g., reported risk levels of COVID-19. Bayesian STVC series models were extended not only to achieve the estimation of PRPI but also to successfully reveal the existence of significant spatiotemporal disparities both in regional public attention to COVID-19 and in its associations with influencing factors during China's pandemic wave at national, provincial, and city levels. Multi-level spatiotemporal findings highlighted the importance of formulating varying and precise health promotion strategies to mitigate the ongoing COVID-19 pandemic. Understanding the extent to which the collective public at the fine-scale level responded to the COVID-19 pandemic from both spatial and temporal dimensions is expected to support proactive public relations and social mobilization strategies [78,79]. The key contributions of this work are elaborated and

discussed hereafter.

First, the proposed regional public risk perception index (PRPI) serves as a comprehensive indicator reflecting regional human health attention to COVID-19, due to it highlighting the local associations between collective public attention and actual pandemic risk level from a spatiotemporal heterogeneous perspective. We demonstrated that the actual local risk of COVID-19 had a dominant influence on the online public attention in China [39,40], so it is unreasonable to use only regional public attention to represent collective health behavioral responses or collective health literacy. Traditional indicators of public risk perception based on questionnaires or interviews are difficult to be implemented within every fine-scale region of a large study area [35,36]. The proposed regional PRPI overcomes these limitations. Through cluster and outlier analysis for regional PRPI, we can further identify four types of zones that may require different targeting strategies. Across 366 Chinese cities, overall, less than 10% of cities showed abnormal public risk perception (potential public panic areas and potential low health literacy areas), with most showing normal and stable responses. In practical work, we can use the total PRPI map to facilitate policy interventions at a higher administrative level, the residual PRPI map to identify specific areas where local containment strategies are needed, and the time-varying PRPI maps to provide real-time support for routine containment as the COVID-19 pandemic periodically deteriorates. The regional PRPI provides a fast-response and dynamic-change geospatial way to inform the governments to take local actions in response to major emergencies from a public perspective.

Second, we showed that incorporating the scientific research perspectives of spatiotemporal heterogeneity and multiscale effects are important and helpful for risk management of major emergencies like COVID-19 and interdisciplinary fields, such as infodemiology and infoveillance [20]. Uniform and one-size-fits-all public health interventions could be ineffective and costly in containing the COVID-19 pandemic [27,28,80]. Our discoveries of spatiotemporal disparities in China suggested that a science-based guideline should consider collective public demands and be tailored to both local conditions and changing circumstances to provide immediate and precise actions responding to COVID-19 [31,33]. COVID-19 studies on NPIs and vaccination performed at a national level should also be cautiously interpreted when downscaled to regional and local levels [81]. This study not only reveals the necessity of spatiotemporal heterogeneity but also demonstrates the importance of multiscale effects in regional public concern and risk perception surveys. During the COVID-19 pandemic, local prevention strategies can be effective in many aspects on a smaller scale of geographic administrative division; however, implementing these local strategies would require substantial input in labor forces, health care resources, and social coordination [79]. In order to better allocate and manage public attention resources, we designed a multi-level spatiotemporal heterogeneous analytical framework to support the cost-effective idea that higher-level organizations provide overarching guidelines while allowing lower-level organizations to design different policies. In China, for example, paying attention to national-level public dynamics alone was not enough to fully understand COVID-19 due to substantial spatiotemporal disparities discovered among cities and provinces in this work. Among them, the provincial-level spatiotemporal effects accounted for 81.9% of variations in Chinese cities' regional public attention. Even after adjusting provincial time-varying impacts, the city-specific effects accounted for 58.6% of regional public risk perception variations. Reference to public information only at the national or provincial level may lead to uncertainties or unsuccessful pandemic prevention policies [15]. For all these reasons, we recommend a multi-level response system for major emergencies, such as cities with a high level of irregular heterogeneity being considered separately, whereas most cities with uniform or clustered patterns can be controlled through provincial or national measures to reduce the social and financial burdens posed on the public.

Third, across the globe and in different developing and developed countries, previous studies not only confirmed that internet search data such as Google Trends and Baidu Index had a significant correlation with the real-time number of COVID-19 reported cases [12], but also that many countries failed to take advantage of public attention in the early stage of the pandemic, resulting in more severe outbreaks [9,10]. Our study reached similar conclusions under China's context [39,40] at the urban scale from an integrated perspective of time and space. Despite COVID-19 response strategies vary from country to country, all governments require close attention to public awareness, risk perception, attitudes, opinions, and sentiments [9]. Over the past two years, the COVID-19 pandemic has gone through different phases, and accordingly, the factors influencing public attention are constantly changing. Until May 2022, as the COVID-19 pandemic entered the Omicron phase, the up-to-date internet search keywords and influence factors will likely focus on vaccines (third and fourth injections), self-testing, and home-based testing to better evaluate the current regional online public attention to COVID-19 for both developing and developed countries [82,83]. Encouragingly, the method innovatively proposed in this study for identifying the spatiotemporal disparities of both regional public attention and regional public risk perception is applicable to all countries and regions.

Fourth, in terms of methodologies, we officially proposed the series models of Bayesian STVC, so far covering STVC [49,50], STIVC, STVI, and STIVI, as a new kind of spatiotemporal non-stationary regression approach that can be widely used to explore spatiotemporally varying and multi-level relationships of variables, including temporal, spatial, and spatiotemporal interaction heterogeneity. Bayesian STVC series models are designed within the real full-map Bayesian hierarchical modeling framework with flexibility in model extensibility [50,63,64]. The STVC and STIVC models are the two cores of Bayesian STVC series modeling, which are based on the non-stationary assumptions of spatiotemporal independence and spatiotemporal interaction, respectively. Compared with the previous STVC model, in addition to considering space–time interactions, another advantage of the improved STIVC model resides in its flexibility in analyzing complex space–time coupling data organized in two levels, such as counties/cities within states/provinces at the space scale [74], or days/seasons within months/years at the time scale. Moreover, through introducing spatial (or temporal) stratified heterogeneity to define the spatiotemporal interaction non-stationarity, the STIVC model not only ensures the proper complexity of the model and the feasibility of Bayesian inference and improves model fit and prediction ability, but also avoids the over-fitting problem of an SLH-level spatiotemporal interaction non-stationary regression [50]. In contrast, the STVI and STIVI models serve as two simplified versions of the STVC and STIVC models without considering any non-stationary effects of covariates and are

thus used only to fit the multiscale spatiotemporal variation towards the target variable [58,67]. For this COVID-19 case, Bayesian STVC series models were successfully used to achieve the spatiotemporal analysis of the description and influencing factors for regional public attention and to further estimate the regional PRPI for advanced cluster and outlier mapping analysis to identify sensitive areas. A multi-level spatiotemporal heterogeneous analytical framework was also well designed by taking advantage of the Bayesian STVC series modeling to assist in coming up with spatially targeted and rapidly changing strategies for the ongoing COVID-19 pandemic and major emergencies in the future.

Lastly, to overcome the limitations of this study, future studies could improve the understanding of how regional public attention and risk perception interact with NPIs, vaccines, and other emerging strategies in containing COVID-19. First, the public health crisis may arouse a positive public response to NPIs and disruptive emotions against those strategies [15]. In this study, we did not separate these different attitudes toward COVID-19 due to the original limitations embedded in the internet search engine data. As more information has been released through social media, the overall public responses to the pandemic largely supported the NPIs in China [42,84]. For future studies in countries where mixed public responses were previously identified, we suggest that social media complement the internet search engine data to investigate regional public responses and behaviors [15,17,85]. Second, this study mainly focused on the nationwide wave of the pandemic in China when the vaccines for SARS-CoV-2 were not available. Therefore, we did not explore how regional public risk perception was altered by rapid vaccination in China, and the regional public attention might drop due to high vaccination coverage rates and lifted NPIs. Choosing different search keywords on testing or vaccination will be an essential topic requiring further investigation [82,86]. Third, as regional collective efficacy, including regional public risk perception, played an essential role in shaping the spread of COVID-19, our findings may be used to guide immediate actions for the ongoing pandemic. Regional spatiotemporal scale information relevant to the public can serve as viable modeling inputs for assessing infection transmission and the effectiveness of regional NPIs within a country and worldwide. Finally, the regional PRPI could be extended to consider more attribute dimensions to reflect collective public health behaviors more comprehensively and specifically [35,36].

## 5. Conclusions

Using Bayesian STVC series models to focus on a multi-level spatiotemporal heterogeneous perspective, we presented the first study to demonstrate the significant spatiotemporal disparities towards associations of regional internet public attention with its influencing factors across 366 cities during the first COVID-19 pandemic wave in China. Uniform COVID-19 mitigation strategies concerning public attention and risk perception are not adequate for all cities within China. The regional public risk perception index (PRPI) identified abnormal regions with insufficient or excessive attention by integrating the areal public attention data with local infection risks to inform targeted subnational intervention strategies. Some cities seemed to overreact to the pandemic and might implement excessive interventions, while some other cities might show low-level responses while the infection risk level was higher than what they perceived. PRPI is effective in identifying sensitive regions to improve collective human responses in front of major emergencies and disasters. The spatiotemporal heterogeneity in regional public risk perception highlights the importance of localized information to guide effective containment strategies. The national, provincial, and city-level findings from China further revealed that it is necessary to establish collaborations and coordination between national and subnational governments to facilitate effective responses to the spread of infections. More importantly, we proposed Bayesian STVC series models systematically for the first time, aiming to analyze complex spatiotemporal heterogeneous associations between the target variable and various explanatory variables in the real world, which can be applied in broader nature and social sciences to solve space–time scale issues related to description, influencing factor analysis, and prediction.

## Funding

This work was supported by the National Natural Science Foundation of China [grant numbers 42071379, 71874116, 72074163, 71904104, 72104159, 41701448]; the Sichuan Science and Technology Department [grant numbers 2022YFS0052, 2021YFQ0060, 2020YJ0117]; the Chongqing Science and Technology Bureau [grant number cstc2020jscx-cylhX0001]; the Medical Science and Technology Project of Sichuan Provincial Health Commission [grant number 21PJ067]; the Sichuan Provincial Health Commission Project for Prevention and Treatment of Major Infectious Diseases [grant number 2021zc01]; the Fund for Introducing Talents of Sichuan University [grant number YJ202157]; the Research Center of Sichuan County Economy Development [grant number xy2021018]; and the Chengdu Federation of Social Science Association [grant number 2021ZC003]. The funders had no role in the study design, data collection, analysis, publishing decision, or manuscript preparation.

## Declaration of competing interest

The authors declare that they have no known competing financial interests or personal relationships that could have appeared to influence the work reported in this paper.

## Acknowledgments

We are grateful to Henry Chung (Michigan State University, US) for his ongoing language and academic writing assistance. We appreciate Håvard Rue (King Abdullah University of Science and Technology, Norway), the leading developer of the R-INLA project. We also thank the editors and anonymous reviewers for their constructive comments and valuable suggestions on improving our manuscript.

## Appendix A. Supplementary data

Supplementary data to this article can be found online at https://doi.org/10.1016/j.ijdrr.2022.103078.

## References


[1] J. Wang, et al., Influencing factors for public risk perception of COVID-19——perspective of the pandemic whole life cycle, Int. J. Disaster Risk Reduc. 67 (2022) 102693.
[2] M.A. Chisty, et al., Risk perception and information-seeking behavior during emergency: an exploratory study on COVID-19 pandemic in Bangladesh, Int. J. Disaster Risk Reduc. 65 (2021) 102580.
[3] H. Tian, et al., An investigation of transmission control measures during the first 50 days of the COVID-19 epidemic in China, Science 368 (6491) (2020) 638–642.
[4] Q. Li, et al., Early transmission dynamics in Wuhan, China, of novel coronavirus–infected pneumonia, N. Engl. J. Med. 382 (13) (2020) 1199–1207.
[5] S. Flaxman, et al., Estimating the effects of non-pharmaceutical interventions on COVID-19 in Europe, Nature 584 (7820) (2020) 257–261.
[6] S. Lai, et al., Effect of non-pharmaceutical interventions to contain COVID-19 in China, Nature 585 (7825) (2020) 410–413.
[7] Y. Ge, et al., Impacts of worldwide individual non-pharmaceutical interventions on COVID-19 transmission across waves and space, Int. J. Appl. Earth Obs. Geoinf. 106 (2022) 102649.
[8] B. Huang, et al., Integrated vaccination and physical distancing interventions to prevent future COVID-19 waves in Chinese cities, Nat. Human Behav. (2021) 1–11.
[9] Z. Hou, et al., Cross-country comparison of public awareness, rumors, and behavioral responses to the COVID-19 epidemic: infodemiology study, J. Med. Internet Res. 22 (8) (2020) e21143.
[10] D. Hu, et al., More effective strategies are required to strengthen public awareness of COVID-19: evidence from Google Trends, J. Global Health 10 (1) (2020).
[11] A. Masrur, et al., Space-time patterns, change, and propagation of COVID-19 risk relative to the intervention scenarios in Bangladesh, Int. J. Environ. Res. Publ. Health 17 (16) (2020) 5911.
[12] M. Effenberger, et al., Association of the COVID-19 pandemic with internet search volumes: a Google TrendsTM analysis, Int. J. Infect. Dis. 95 (2020) 192–197.
[13] A.I. Bento, et al., Evidence from internet search data shows information-seeking responses to news of local COVID-19 cases, Proc. Natl. Acad. Sci. Unit. States Am. 117 (21) (2020) 11220–11222.
[14] E. Dong, H. Du, L. Gardner, An interactive web-based dashboard to track COVID-19 in real time, Lancet Infect. Dis. 20 (5) (2020) 533–534.
[15] Y. Yang, et al., Spatial evolution patterns of public panic on Chinese social networks amidst the COVID-19 pandemic, Int. J. Disaster Risk Reduc. (2022) 102762.
[16] R.C. Chick, et al., Using technology to maintain the education of residents during the COVID-19 pandemic, J. Surg. Educ. 77 (4) (2020) 729–732.
[17] S.F. Tsao, et al., What Social Media Told Us in the Time of COVID-19: a Scoping Review, The Lancet Digital Health, 2021.
[18] J. Ginsberg, et al., Detecting influenza epidemics using search engine query data, Nature 457 (7232) (2009) 1012–1014.
[19] G.J. Milinovich, et al., Internet-based surveillance systems for monitoring emerging infectious diseases, Lancet Infect. Dis. 14 (2) (2014) 160–168.
[20] G. Eysenbach, Infodemiology and infoveillance: tracking online health information and cyber behavior for public health, Am. J. Prev. Med. 40 (5) (2011) S154–S158.
[21] Y. Dai, J. Wang, Identifying the outbreak signal of COVID-19 before the response of the traditional disease monitoring system, PLoS Neglected Trop. Dis. 14 (10) (2020) e0008758.
[22] I. Husain, et al., Fluctuation of public interest in COVID-19 in the United States: retrospective analysis of google trends search data, JMIR Publ. Health Surv. 6 (3) (2020) e19969.
[23] L.J. Thomas, et al., Spatial heterogeneity can lead to substantial local variations in COVID-19 timing and severity, Proc. Natl. Acad. Sci. Unit. States Am. 117 (39) (2020) 24180–24187.
[24] Y. Ma, et al., Role of meteorological factors in the transmission of SARS-CoV-2 in the United States, Nat. Commun. 12 (1) (2021) 1–9.
[25] W.A. Chiu, R. Fischer, M.L. Ndeffo-Mbah, State-level needs for social distancing and contact tracing to contain COVID-19 in the United States, Nat. Human Behav. 4 (10) (2020) 1080–1090.
[26] H.J.T. Unwin, et al., State-level tracking of COVID-19 in the United States, Nat. Commun. 11 (1) (2020) 1–9.
[27] S. Mehtar, et al., Limiting the spread of COVID-19 in Africa: one size mitigation strategies do not fit all countries, Lancet Global Health 8 (7) (2020) e881–e883.
[28] E.H. Bradley, M.W. An, E. Fox, Reopening colleges during the coronavirus disease 2019 (COVID-19) pandemic—one size does not fit all, JAMA Netw. Open 3 (7) (2020) e2017838-e2017838.
[29] S. Pei, et al., Burden and characteristics of COVID-19 in the United States during 2020, Nature 598 (7880) (2021) 338–341.
[30] C. Yang, et al., Taking the pulse of COVID-19: a spatiotemporal perspective, Int. J. Digit. Earth 13 (10) (2020) 1186–1211.
[31] Y. Wang, et al., Spatiotemporal characteristics of the COVID-19 epidemic in the United States, Clin. Infect. Dis. 72 (4) (2021) 643–651.
[32] A. Mollalo, B. Vahedi, K.M. Rivera, GIS-based spatial modeling of COVID-19 incidence rate in the continental United States, Sci. Total Environ. 728 (2020) 138884.
[33] A. Maiti, et al., Exploring spatiotemporal effects of the driving factors on COVID-19 incidences in the contiguous United States, Sustain. Cities Soc. 68 (2021) 102784.
[34] X. Wu, et al., Natural and human environment interactively drive spread pattern of COVID-19: a city-level modeling study in China, Sci. Total Environ. 756 (2021) 143343.
[35] S. Dryhurst, et al., Risk perceptions of COVID-19 around the world, J. Risk Res. 23 (7–8) (2020) 994–1006.
[36] Y. Chen, et al., Risk perception of COVID-19: a comparative analysis of China and South Korea, Int. J. Disaster Risk Reduc. (2021) 102373.
[37] M. Ye, Z. Lyu, Trust, risk perception, and COVID-19 infections: evidence from multilevel analyses of combined original dataset in China, Soc. Sci. Med. 265 (2020) 113517.
[38] M. Siegrist, A. Bearth, Worldviews, trust, and risk perceptions shape public acceptance of COVID-19 public health measures, Proc. Natl. Acad. Sci. Unit. States Am. 118 (24) (2021).
[39] C. Xu, X. Zhang, Y. Wang, Mapping of health literacy and social panic via web search data during the COVID-19 public health emergency: infodemiological study, J. Med. Internet Res. 22 (7) (2020) e18831.
[40] X. Gong, et al., Online public attention during the early days of the COVID-19 pandemic: infoveillance study based on Baidu index, JMIR Publ. Health Surv. 6 (4) (2020) e23098.
[41] A.O. Opesade, Discovering patterns in electronic commerce diffusion in Nigeria using Google Trends Web Data, J. Info. Sci. Syst. Technol. 4 (1) (2020) 1–20.
[42] B. Zhu, et al., Analysis of spatiotemporal characteristics of big data on social media sentiment with COVID-19 epidemic topics, Chaos, Solit. Fractals 140 (2020) 110123.
[43] A. Sofi-Mahmudi, et al., Association of COVID-19-imposed lockdown and online searches for toothache in Iran, BMC Oral Health 21 (1) (2021) 1–7.
[44] M. Laszkowska, et al., The Gluten-Free Diet Epidemic: Socioeconomic Factors Predict Google Search Trends More Than Health-Related Factors, Clin. Gastroenterol. Hepatol. 112 (S) (2017) S655–S656, https://doi.org/10.14309/00000434-201710001-01194.
[45] A.K. Monika, The utility of 'covid-19 mobility report'and 'google trend'for analysing economic activities, Syntax Idea 3 (6) (2021) 1256–1268.
[46] T. Hu, et al., Human mobility data in the COVID-19 pandemic: characteristics, applications, and challenges, Int. J. Digit. Earth 14 (9) (2021) 1126–1147.

[47] Y. Sun, et al., Temporal and spatial differences of public attention to COVID-19 and its influencing factors based on Baidu search index, Trop. Geogr. 40 (3) (2020) 375–385, https://doi.org/10.13284/j.cnki.rddl.003244.
[48] J.S. Jia, et al., Population flow drives spatio-temporal distribution of COVID-19 in China, Nature 582 (7812) (2020) 389–394.
[49] C. Song, et al., Exploring spatiotemporal nonstationary effects of climate factors on hand, foot, and mouth disease using Bayesian Spatiotemporally Varying Coefficients (STVC) model in Sichuan, China, Sci. Total Environ. 648 (2019) 550–560.
[50] C. Song, X. Shi, J. Wang, Spatiotemporally Varying Coefficients (STVC) model: a Bayesian local regression to detect spatial and temporal nonstationarity in variables relationships, ANN GIS 26 (3) (2020) 277–291.
[51] D. Huang, J. Wang, Monitoring hand, foot and mouth disease by combining search engine query data and meteorological factors, Sci. Total Environ. 612 (2018) 1293–1299.
[52] L. Zhou, et al., 100 Days of COVID-19 Prevention and Control in China, Clinical Infectious Diseases, 2020.
[53] W. Lieberman-Cribbin, et al., Disparities in COVID-19 testing and positivity in New York City, Am. J. Prev. Med. 59 (3) (2020) 326–332.
[54] T. Wu, et al., nCov 2019: an R package for studying the COVID-19 coronavirus pandemic, PeerJ 9 (2021) e11421.
[55] R.M. O'brien, A caution regarding rules of thumb for variance inflation factors, Qual. Quantity 41 (5) (2007) 673–690.
[56] L. Knorr-Held, Bayesian modelling of inseparable space-time variation in disease risk, Stat. Med. 19 (17-18) (2000) 2555–2567.
[57] J. Wang, T. Zhang, B. Fu, A measure of spatial stratified heterogeneity, Ecol. Indicat. 67 (2016) 250–256.
[58] C. Song, et al., Spatial and temporal impacts of socioeconomic and environmental factors on healthcare resources: a county-level bayesian local spatiotemporal regression modeling study of hospital beds in Southwest China, Int. J. Environ. Res. Publ. Health 17 (16) (2020) 5890.
[59] A. Adin, T. Goicoa, M.D. Ugarte, Online relative risks/rates estimation in spatial and spatio-temporal disease mapping, Comput. Methods Progr. Biomed. 172 (2019) 103–116.
[60] B. Schrödle, L. Held, Spatio-temporal disease mapping using INLA, Environmetrics 22 (6) (2011) 725–734.
[61] B. Huang, B. Wu, M. Barry, Geographically and temporally weighted regression for modeling spatio-temporal variation in house prices, Int. J. Geogr. Inf. Sci. 24 (3) (2010) 383–401.
[62] A.S. Fotheringham, R. Crespo, J. Yao, Geographical and temporal weighted regression (GTWR), Geogr. Anal. 47 (4) (2015) 431–452.
[63] A.O. Finley, Comparing spatially-varying coefficients models for analysis of ecological data with non-stationary and anisotropic residual dependence, Methods Ecol. Evol. 2 (2) (2011) 143–154.
[64] L.J. Wolf, T.M. Oshan, A.S. Fotheringham, Single and multiscale models of process spatial heterogeneity, Geogr. Anal. 50 (3) (2018) 223–246.
[65] P. Moraga, Geospatial Health Data: Modeling and Visualization with R-INLA and Shiny, Chapman and Hall/CRC, 2019.
[66] X. Wang, Y.Y. Ryan, J.J. Faraway, Bayesian Regression Modeling with INLA, Chapman and Hall/CRC, 2018.
[67] X. Zhang, et al., Socioeconomic and environmental impacts on regional tourism across Chinese cities: a spatiotemporal heterogeneous perspective, ISPRS Int. J. Geo-Inf. 10 (6) (2021) 410.
[68] M. Blangiardo, M. Cameletti, Spatial and Spatio-Temporal Bayesian Models with R-INLA, John Wiley & Sons, 2015.
[69] H. Rue, et al., Bayesian computing with INLA: a review, Ann. Rev. Statis. Appl. 4 (2017) 395–421.
[70] W.R. Tobler, A computer movie simulating urban growth in the Detroit region, Econ. Geogr. 46 (sup1) (1970) 234–240.
[71] M.F. Goodchild, The validity and usefulness of laws in geographic information science and geography, Ann. Assoc. Am. Geogr. 94 (2) (2004) 300–303.
[72] J. Besag, Spatial interaction and the statistical analysis of lattice systems, J. Roy. Stat. Soc. B 36 (2) (1974) 192–225.
[73] C. Song, et al., Disease relative risk downscaling model to localize spatial epidemiologic indicators for mapping hand, foot, and mouth disease over China, Stoch. Environ. Res. Risk Assess. 33 (10) (2019) 1815–1833.
[74] M.D. Ugarte, A. Adin, T. Goicoa, Two-level spatially structured models in spatio-temporal disease mapping, Stat. Methods Med. Res. 25 (4) (2016) 1080–1100.
[75] R. Genuer, J.-M. Poggi, C. Tuleau-Malot, Variable selection using random forests, Pattern Recogn. Lett. 31 (14) (2010) 2225–2236.
[76] H. Rue, S. Martino, N. Chopin, Approximate Bayesian inference for latent Gaussian models by using integrated nested Laplace approximations, J. Roy. Stat. Soc. B 71 (2) (2009) 319–392.
[77] L. Anselin, Local indicators of spatial association—LISA, Geogr. Anal. 27 (2) (1995) 93–115.
[78] D.M. Hartley, E.N. Perencevich, Public health interventions for COVID-19: emerging evidence and implications for an evolving public health crisis, JAMA 323 (19) (2020) 1908–1909.
[79] Z. Li, G.F. Gao, Strengthening public health at the community-level in China, Lancet Public Health 5 (12) (2020) e629–e630.
[80] A. Glassman, K. Chalkidou, R. Sullivan, Does one size fit all? Realistic alternatives for COVID-19 response in low-income countries, Cent. Global Dev. 2 (2020).
[81] J. Yang, et al., Despite vaccination, China needs non-pharmaceutical interventions to prevent widespread outbreaks of COVID-19 in 2021, Nat. Human Behav. (2021) 1–12.
[82] A. Hussain, et al., Artificial intelligence–enabled analysis of public attitudes on facebook and twitter toward covid-19 vaccines in the United Kingdom and the United States: observational study, J. Med. Internet Res. 23 (4) (2021) e26627.
[83] C. Zhang, et al., The evolution and disparities of online attitudes toward COVID-19 vaccines: year-long longitudinal and cross-sectional study, J. Med. Internet Res. 24 (1) (2022) e32394.
[84] S. Zhang, et al., Characterizing the COVID-19 infodemic on Chinese social media: exploratory study, JMIR Publ. Health Surv. 7 (2) (2021) e26090.
[85] T. Hu, et al., Revealing public opinion towards COVID-19 vaccines with twitter data in the United States: spatiotemporal perspective, J. Med. Internet Res. 23 (9) (2021) e30854.
[86] S. Yang, et al., Spatial technologies to strengthen traditional testing for SARS-CoV-2, Trends Microbiol. 29 (12) (2021) 1055–1057.